



Investigating the susceptibility of *Enterobacter xiangfangensis* Pb204 to various silver(I) phosphine compounds and identifying the molecular basis of resistance through comparative genomics

By

Phindile Ntuli

(1420924)

Dissertation

Submitted in fulfilment of the requirements for the degree

Master of Science

In

Molecular and Cell Biology

In the Faculty of Science, University of the Witwatersrand, Johannesburg, South

Africa

Supervisor: Prof. M.J. Cronjé

Co-supervisor: Dr. Z. Engelbrecht

October 2023

Declaration

I declare that this dissertation is my own, unaided work. It is being submitted for the Degree of Master of Science at the University of the Witwatersrand, Johannesburg.

It has not been submitted before for any degree or examination at any other University.

A handwritten signature in black ink, appearing to read 'P. M. Muti', written in a cursive style with a long horizontal stroke at the end. The signature is positioned above a solid horizontal line that spans the width of the page.

(Signature of candidate)

16th day of October 2023 at Johannesburg, Gauteng.

DEDICATION

To my grandfather and my late beloved father France Ngwenya.

ACKNOWLEDGEMENTS

- * I thank God for giving me the opportunity to do my MSc degree and for being my comfort in times of distress.
- * Prof. Marianne J. Cronjé for welcoming me into her lab since honors year and allowing me to pursue this research.
- * Dr. Zelinda Engelbrecht for working together with Prof Cronjé to facilitate and provide guidance to make this project possible.
- * I extend my sincere thanks to Prof. Pieter De Maayer who served as my lab advisor. His continued guidance and advice had a great impact on this project.
- * Dr. Vanessa Meyer (along with Prof. Cronjé) for I was able to type this dissertation and do the bioinformatics analysis from the laptop she lent me.
- * Further, the parents who have trusted me to tutor their children. This has been an incredible resource enabling me to support my studies when during a time when I lacked any financial assistance.
- * The NRF for awarding me with the scholarship in the final year of this project.
- * Total SA for covering my tuition fees with their donation.
- * Mufunwa, Elsie, Keelan and colleagues in the Microbiology and Biotechnology department (Wits School of MCB) who have assisted me throughout my degree in the lab.
- * Alisha, thanks for being such an amazing friend your love and support is much appreciated.

Table of Contents

LIST OF FIGURES	vii
LIST OF TABLES	ix
LIST OF ABBREVIATIONS	x
ABSTRACT	xii
CHAPTER ONE: LITERATURE REVIEW	1
1.1 NOSOCOMIAL INFECTIONS	2
1.2 ESKAPE PATHOGENS	3
1.2.1 GRAM-POSITIVE ESKAPE	3
1.2.2 GRAM-NEGATIVE ESKAPE	3
1.3 BACTERIAL BIOFILM	5
1.4 MDR IN ECC	7
1.5 USE OF METALS IN MEDICINE	9
1.5.1 GOLD-BASED COMPLEXES	10
1.5.2 PLATINUM-BASED COMPLEXES	11
1.5.3 SILVER-BASED COMPOUNDS	11
1.6 HEAVY-METAL RESISTANCE IN <i>ENTEROBACTER XIANGFANGENSIS</i> PB204 ..	13
1.7 AIMS AND OBJECTIVES	16
CHAPTER TWO: METHODS AND MATERIALS	17
2.1 MEDIA AND AGAR PREPARATION	18
2.2 BACTERIA CULTURING	18
2.3 PREPARATION OF COMPOUNDS	18
2.4 MINIMUM INHIBITORY CONCENTRATION (MIC) ASSAY	19
2.5 ANTIBIOFILM ASSAY	21
2.5.1 ESTABLISHING A BIOFILM	21
2.5.2 MICROTITER DISH BIOFILM FORMATION ASSAY	22
2.5.2.1 CRYSTAL VIOLET ASSAY	22
2.5.2.2 XTT ASSAY	22
2.6 QUANTITATIVE REVERSE TRANSCRIPTION PCR	23
2.6.1 RNA ISOLATION	23
2.6.1.1 LYSATE PREPARATION FROM BACTERIA	23
2.6.1.2 RNA QUANTITY AND INTEGRITY	25
2.6.2 CDNA SYNTHESIS	25
2.6.3 PRIMER DESIGN	26
2.6.4 QUANTITATIVE REAL-TIME PCR	26
2.7 COMPARATIVE GENOMICS	27

2.7.1 COMPARATIVE GENOMICS ANALYSIS	27
2.8 STATISTICAL ANALYSIS.....	28
CHAPTER THREE: RESULTS	29
3.1 SCREENING THE ANTIMICROBIAL ACTIVITY OF THE SILVER(I) PHOSPHINE COMPOUNDS	30
3.1.1 MINIMUM INHIBITORY CONCENTRATION (MIC)	30
3.1.2 MINIMUM BACTERICIDAL CONCENTRATION (MBC).....	33
3.2 INVESTIGATING THE ANTI-BIOFILM ACTIVITY OF THE SILVER(I) PHOSPHINE COMPOUNDS.....	37
3.2.1 CRYSTAL VIOLET ASSAY	37
3.2.2 XTT ASSAY	41
3.3 GENE EXPRESSION STUDIES	44
3.4 COMPARATIVE GENOMICS.....	46
CHAPTER FOUR: DISCUSSION.....	50
4.1 ANTIBACTERIAL ACTIVITY OF SILVER(I) PHOSPHINE COMPOUNDS	51
4.2 ANTIBIOFILM ACTIVITY	53
4.3 SILVER RESISTANCE PATHWAY	55
4.4 COMPARATIVE GENOMICS.....	56
CHAPTER FIVE: CONCLUSION	58
5.1 CONCLUSION	59
5.2 FUTURE STUDIES	59
REFERENCES.....	61
APPENDIX A	74
A1.1 CHARACTERIZATION OF COMPOUNDS	74
Synthesis of UJ1: Silver(I) bromide triphenylphosphine [AgBr {(PPh ₃) ₃ }] - batch A21	75
Synthesis of UJ2: Silver(I) chloride tris(4-chlorophenyl) phosphine [AgCl {(pClC ₆ H ₄) ₃ P}] ₃ - batch A31	76
Synthesis of UJ3: Silver(I) thiocyanate 4-methoxyphenyl phosphine [AgSCN{P(4- MeOC ₆ H ₄) ₃ }] ₂ – batch A64	77
Synthesis of UJ4: Silver(I) nitrate tris(4-chlorophenyl) phosphine [AgNO ₃ {(pClC ₆ H ₄) ₃ P}] ₃ - batch A42	78
Synthesis of UJ1A: Silver(I) bromide tri(p-tolyl)phosphine [AgBr(4-CH ₃ PPh ₃) ₃] - batch A45	79
Synthesis of UJ15: Silver(I) nitrate tri(p-tolyl)phosphine [AgNO ₃ (4-CH ₃ PPh ₃) ₃]	80
Synthesis of UJ34: Silver(I) nitrate triphenylphosphine [AgNO ₃ (PPh ₃) ₂] – batch A18	81

Synthesis of UJ35: Silver(I) thiocyanide tris(4-chlorophenyl) phosphine [AgSCN(pClC₆H₄)₃P]₂.....	82
APPENDIX B	84
B1.1 REAL-TIME QUANTITATIVE PCR DATA.....	84

LIST OF FIGURES

Figure 1.1: Schematic diagram depicting the variance between the outer membrane of Gram-positive and Gram-negative bacteria. The Gram-negative bacteria comprise of a thick outer membrane which is bounded by a lipopolysaccharide layer, the Gram-positive bacteria have a thin membrane which lacks the lipopolysaccharide (Adapted from Steward (2022)).	4
Figure 1.2: Diagrammatic depiction of biofilm formation in microorganisms (Prakash <i>et al.</i> , 2003).	6
Figure 1.3: Schematic representation of five major efflux pumps family in bacteria (Adapted from Blanco <i>et al.</i> (2016)).	8
Figure 1.4: Schematic diagram of ICEExiPb204. The genes for the silver, gold, zinc, arsenic and copper resistance pathways are shown. Green arrows signify the integration, excision, and maintenance of ICE-related proteins. Yellow arrows denote genes involved in DNA damage SOS response (umuDC). Transposons and genes coding for hypothetical proteins are shown in black and white (Adapted from Ho <i>et al.</i> (2018)).	15
Figure 2.1: Template illustrating how the 96-well plates were prepared and the concentration range used for MIC studies for the broth dilution method. Serial dilutions of the compounds (silver(I) or positive controls silver nitrate and silver sulfadiazine) were done on the <i>Enterobacter xiangfangensis</i> pathogens. In addition, a positive untreated, negative media control and vehicle control, 25% DMSO was also included. A total of eight different silver (I) phosphine compounds were tested, and 4 compounds were serially diluted in one plate (the colours on the plate indicate different treatments used).	20
Figure 3.1: The inhibitory effects of various silver(I) phosphine complexes on <i>Enterobacter xiangfangensis</i> Pb204 and <i>Enterobacter xiangfangensis</i> LMG 27195 ^T biofilm formation when co-incubated for 48 h at their respective MIC concentrations. The DMSO (25%) was used as a vehicle control and the percentage biofilm formation for each treatment were calculated with reference to the vehicle control. Silver sulfadiazine and silver nitrate salts (positive antimicrobial controls) were used. The error bars represent the standard error of mean (SEM; n = 9). The significant difference between the treated samples and the vehicle control were calculated using the student t-test (*** p < 0.001).	38
Figure 3.2: The effect of the silver(I) phosphine compounds on matured biofilms formed by <i>Enterobacter xiangfangensis</i> Pb204 and <i>Enterobacter xiangfangensis</i> LMG. The biofilms were allowed to form in 48 h, thereafter, treated with the various silver(I) phosphine compounds, silver nitrate and silver sulfadiazine were used as positive control, and the untreated biofilms were regarded as negative control. The percentage biofilm degradation was calculated with respect to the vehicle control DMSO (25%). The error bars represent the SEM (n = 9) and the significance difference is represented with an asterik (** p<0.01, *** p<0.001).	40

Figure 3.3: The metabolic activity of *Enterobacter xiangfangensis* Pb204 and *Enterobacter xiangfangensis* LMG 27195^T biofilms when co-incubated with different silver phosphine compounds. The untreated control, silver nitrate and silver sulfadiazine positive controls, and DMSO (25%) vehicle control was included. The cells were co-incubated with the treatments for 48 h to allow biofilm formation to take place. The percentage metabolic activity was calculated relative to DMSO (25%) vehicle control. The error bars represent the standard error of mean (SEM, where n = 9). The significance difference between the DMSO(25%) vehicle control and treated samples was calculated using the student's t-test (** p<0.01).....42

Figure 3.4: Metabolic activity of *Enterobacter xiangfangensis* Pb204 and *Enterobacter xiangfangensis* LMG 27195^T 48 h formed biofilms when treated with various silver(I) phosphine compounds at their MIC (and the controls). Silver nitrate and silver sulfadiazine were used as positive controls, untreated cells were included as negative control. Metabolic activity is conveyed as percentage relative to the vehicle control (25% DMSO). The standard error of mean (SEM; n = 9) is presented as error bars. The significant difference was calculated using the student's t-test (*** p<0.001).....43

Figure 3.5: Log Fold gene expression of the different genes (*silA*, *silR*, *silS*) encoded on the ICE element which codes for the activation of the silver resistance pathway in *Enterobacter xiangfangensis* Pb204. The cells were treated with UJ1 compound, AgSD and AgNO₃ salts. The $\Delta\Delta Ct$ method was used to calculate the fold gene expression with respect to DMSO. The error bars signify the standard error of mean (SEM; n = 6).....45

Figure 3.6: Venn diagram showing proteins that are shared (core proteins) between the two *Enterobacter xiangfangensis* strains and proteins that are unique to each strain. The orthologous proteins were analysed using OrthoFinder.....46

Figure 3.7: COG Classification of core and unique proteins encoded in the genomes of the compared *Enterobacter xiangfangensis* Pb204 and *Enterobacter xiangfangensis* LMG 27195^T. The eggNOG mapper server was used.....47

Figure 3.8: Number of core and unique proteins encoded on the genomes of *Enterobacter xiangfangensis* Pb204 and *Enterobacter xiangfangensis* LMG 27195^T involved in metabolism, information storage and processing, as well as cellular processes and signalling functional categories.....48

Figure A1.1: Chemical structure of UJ1 (Jenkins, 2014, Ferreira, 2023).....75

Figure A1.2: Chemical structure of UJ2 (Engelbrecht, 2017; Mizan, 2023).....76

Figure A1.3: Chemical structure of UJ3 (Ferreira *et al.*, 2015; Engelbrecht *et al.*, 2018).....77

Figure A1.4: Chemical structure of UJ4 (Engelbrecht, 2017).....78

Figure A1.5: Chemical structure of UJ1A (Engelbrecht, 2017).....79

Figure A1.6: Chemical structure of UJ15 (Engelbrecht, 2017).....	80
Figure A1.7: Chemical structure of UJ34 (Engelbrecht <i>et al.</i> ,2018b).....	81
Figure A1.8: Chemical structure of UJ35 (Ferreria <i>et al.</i> , 2015; Human <i>et al.</i> , 2015).....	82
Figure A2.1: Agarose gel (1%) showing the integrity of RNA extracted from <i>Enterobacter xiangfangensis</i> Pb204 cells treated with UJ1, silver nitrate and silver sulfadiazine. The cells were treated for 16 h prior to RNA extraction. The intact 23S and 16S unit is shown on each lane.....	84

LIST OF TABLES

Table 2.1: Primer sequences for specific genes coding for the silver resistance pathway as well as the housekeeping gene (<i>gyrB</i>).....	26
Table 3.1: The minimum inhibitory concentration (MIC) of eight various silver(I) phosphine compounds, AgNO ₃ and AgSD (positive control antimicrobial controls) against <i>Enterobacter xiangfangensis</i> Pb204 and <i>Enterobacter xiangfangensis</i> LMG 27195 ^T	32
Table 3.2: The Minimum bactericidal concentration (MBC) of eight different silver(I) phosphine complexes, the silver salt controls (silver nitrate and silver sulfadiazine) against <i>Enterobacter xiangfangensis</i> Pb204 and <i>Enterobacter xiangfangensis</i> LMG 27195 ^T	34
Table 3.3: The minimum bactericidal concentration/minimum inhibitory concentration ratio and the antibacterial effect of silver(I) phosphine compounds and the positive control silver salts against <i>Enterobacter xiangfangensis</i> LMG 27195 ^T	35
Table 3.4: The minimum bactericidal concentration/minimum inhibitory concentration ratio and antibacterial effects of silver(I) phosphine compounds and the positive control silver salts against the <i>Enterobacter xiangfangensis</i> Pb204.....	36
Table B1.1 Concentration and absorbance ratios of RNA extracted from <i>E. xiangfangensis</i> Pb204 treated with silver(I) compounds.....	84

LIST OF ABBREVIATIONS

ABC: ATP-binding cassette

AMR: Antimicrobial resistance

AST: Antibiotic susceptibility testing

AuSR: Gold (I) thiolates

BCCM: Belgian coordinated collections of microorganisms

cDNA: complementary deoxyribonucleic acid

CLSI: Clinical and Laboratory Standards Institute

COD: Cyclooctadiene

CRE: Carbapenem-resistant *Enterobacteriaceae*

CRKP: Carbapenem-resistant *K. pneumoniae*

CV: Crystal violet

DMSO: Dimethyl sulfoxide

ECC: *Enterobacter cloacae* complex

EPS: Extracellular polymeric substances

ESBL: Extended-spectrum β -lactamase

gDNA: genomic deoxyribonucleic acid

HAI: Hospital-acquired infection

ICE: Integrative and conjugative element

ICU: Intensive Care Unit

LB: Luria-Bertani

MATE: Multidrug resistance and toxic compound extrusion

MBA: Metal-based antimicrobials

MBC: Minimum Bactericidal Concentration

MDR: Multidrug resistant

MF: Major facilitator

MGE: Mobile-genetic elements

MIC: Minimal inhibitory concentration

MRSA: Methicillin-resistant *Staphylococcus aureus*

NGS: Next-generation sequencing

NOGs: non-supervised orthologous groups

PBS: Phosphate buffered saline.

RA: Rheumatoid arthritis

RND: Resistance-nodulation-division

RT-qPCR: Reverse transcription-quantitative polymerase chain reaction

SBS: Sequencing by synthesis

SEM: Standard Error of Mean

SilA: Cation efflux system protein

SilR: Transcriptional regulatory protein

SilS: Sensor kinase

SMR: Small multidrug resistance

UTI: Urinary tract infection

VHA: Veterans' Health Administration

VRE: Vancomycin resistant enterococci

WGS: Whole genome sequencing

XTT: 2,3-Bis- (2-Methoxy-4-Nitro-5-Sulfophenyl) -2H-Tetrazolium-5-Carboxanilide

ABSTRACT

In developing countries, the endemic of nosocomial infections is notably high, particularly in the ICU settings and neonatal infections, where it accounts for a prevalence of 15.5% with an increased mortality rate. ESKAPE (*Enterococcus faecium*, *Staphylococcus aureus*, *Klebsiella pneumoniae*, *Acinetobacter baumannii*, *Klebsiella pneumoniae*, *Acinetobacter baumannii*, *Pseudomonas aeruginosa* and *Enterobacter* species) pathogens are highly virulent and resistant microbes that predominantly causes nosocomial infections in clinical settings. These pathogens adhere to the surface of hospital equipment and form biofilms, thereby increasing the susceptibility of patients to acquiring such infections during extended hospital stays. Recent studies have shown that *Enterobacter xiangfangensis* is the main clinical culprit in the *Enterobacter cloacae* complex, thus making it the main therapeutic target among the ESKAPE pathogens. This study evaluated the antimicrobial properties of various silver(I) phosphine compounds on *E. xiangfangensis* Pb204 and *E. xiangfangensis* LMG 27195^T. The minimum inhibitory concentration (MIC) assay was done, though the microdilution technique coupled with iodinitrotetrazolium chloride (INT) dye. The antibiofilm activity of the silver(I) phosphine compounds on biofilm formation and degradation were evaluated using the crystal violet assay, and the metabolic activity of cells in biofilms was assessed using the XTT assay. Additionally, the molecular mechanism of silver resistance was investigated by measuring gene expression of *E. xiangfangensis* Pb204 cells when treated with the silver(I) phosphine compound UJ1, silver nitrate and silver sulfadiazine using RT-qPCR. The MIC of the silver(I) phosphine compounds was 0.125 mg/ml for both *E. xiangfangensis* Pb204 and *E. xiangfangensis* LMG 27195^T. Moreover, the compound UJ1 showed a bactericidal effect against *E. xiangfangensis* LMG 27195^T. Furthermore, the silver(I) phosphine compounds have antibiofilm activity since they inhibit biofilm formation, disrupt matured biofilms, and reduce metabolic activity in *E. xiangfangensis* Pb204 and *E. xiangfangensis* LMG 27195^T biofilms. The resistance in *E. xiangfangensis* Pb204 strain is due to the upregulation of the silver resistance pathway encoded on the integrative and conjugative element (ICE) element. Core and unique protein coding genes between *E. xiangfangensis* Pb204 and *E. xiangfangensis* LMG 27195^T were identified though comparative genomics. Functional annotation of core and unique protein revealed that *E. xiangfangensis* Pb204 evolved to gain genetic material coding for inorganic ion transport and carbohydrate transport metabolism. Knowledge of

these can be used in future studies in the utilization of silver metals as antimicrobial agents.

CHAPTER ONE: LITERATURE REVIEW

1.1 NOSOCOMIAL INFECTIONS

Healthcare-associated infections (HAIs) commonly known as nosocomial infections are often acquired in hospitals due to prolonged stays (Dell *et al.*, 2020). There are different types of HAIs including ventilator-associated pneumonia (VAP), surgical site infections (SSI), central line-associated bloodstream infections (CLABSI), catheter-associated urinary tract infections (CAUTI) and occupational infections (Sikora and Zaha, 2022). In acute hospital settings pneumonia, gastrointestinal, bloodstream and urinary tract infections (UTI) are the most habitual nosocomial infections (Lowman, 2016). Patients with an injured intubation or respiratory system are more prone to pneumonia. SSI are the third most common HAIs in surgical settings, and it is one of the major causes of death in developing countries, with the global rate between 2.5 and 41% (Khan *et al.*, 2017). SSI commonly arise at the site of the surgical procedure and when patients experience such infections, their risk of mortality increases by 11%. Individuals in the intensive care units (ICU) and newborn infants exhibit a higher susceptibility to these infections (Scherbaum *et al.*, 2014).

Bacteria, viruses, and fungi are the main microbes that cause HAIs. However, bacterial pathogens, specifically ESKAPE (*Enterococcus faecium*, *Staphylococcus aureus*, *Klebsiella pneumoniae*, *Acinetobacter baumannii*, *Klebsiella pneumoniae*, *Acinetobacter baumannii*, *Pseudomonas aeruginosa* and *Enterobacter* pathogens), are the most common causative agents of HAIs (Scherbaum *et al.*, 2014). The occurrence of multidrug resistance (MDR) in ESKAPE pathogens makes it difficult to treat HAIs. Therefore, these infections remain a global threat since they contribute to increased mortality and morbidity, they also pose a financial burden on the healthcare system and families (Inweregbu *et al.*, 2005). The endemic occurrence of HAIs is more significant in developing countries, with a prevalence of 15.5% of neonatal infections in ICU settings (Sikora and Zaha, 2022). To facilitate the development of novel antimicrobial drugs, the world health organization (WHO) compiled a list of microorganisms that should be prioritized for antibiotic research. On this list, the ESKAPE pathogens were rated as "priority" (Ramsamy *et al.*, 2018).

1.2 ESKAPE PATHOGENS

1.2.1 GRAM-POSITIVE ESKAPE

The term ESKAPE is used to delineate a group of virulent multidrug-resistant Gram-negative and Gram-positive bacteria accountable for severe infections (Llaca-Díaz *et al.*, 2012). The ESKAPE group consists of Gram-positive bacteria which includes *E. faecium* and *S. aureus*. Generally, *E. faecium* is a round, Gram-positive bacterium seen in groups or pairs (Oliveira *et al.*, 2020). It is resistant to vancomycin and other β -lactam antibiotics, such as penicillin. Vancomycin resistant enterococci (VRE) strains often possess virulent factors that augment their growth such as the ability to form thicker biofilms (Karlowsky *et al.*, 2017). Furthermore, the VRE strains are prone to horizontal gene transfer that spreads their resistance (Tuttobene *et al.*, 2021). *Staphylococcus aureus* forms part of the skin microbiota in humans. Unless it enters a part of the body where it is not supposed to be, such as wounds, it usually does not harm the body (Tuttobene *et al.*, 2021). Moreover, these strains can secrete exotoxins that can cause necrotic haemorrhagic pneumonia and toxic shock syndrome (Ma *et al.*, 2020).

1.2.2 GRAM-NEGATIVE ESKAPE

The Gram-negative ESKAPE includes *K. pneumoniae*, *A. baumannii*, *P. aeruginosa* and *Enterobacter* species (Tuttobene *et al.*, 2021). Known primarily for its resistance to phagocytic treatment, *K. pneumoniae* is a rod-shaped Gram-negative bacterium (Ma *et al.*, 2020). Moreover, several strains have been reported to be resistant to β -lactam antibiotics. To treat the β -lactam resistant strains, carbapenems have been excessively used which led to the development of carbapenem-resistant *K. pneumoniae* (CRKP) which currently cannot be treated with any of the commercially available antibiotics (Mezzatesta *et al.*, 2012). *Acinetobacter baumannii* is a short-rod-shaped coccobacillus found mostly in hospitals. This Gram-negative species' outer membrane and efflux pump aid in its resistance to most antibiotics (Karlowsky *et al.*, 2017). *Pseudomonas aeruginosa* also have highly upregulated efflux pumps that assist them in resisting antibiotics. Additionally, *P. aeruginosa* can usually survive in extreme conditions, so they typically infect late-stage cystic fibrosis patients' lungs (Nikaido, 2009).

The Gram-negative bacteria are the most virulent and resistant to most available antibiotics since they have a thicker outer membrane (Nikaido, 2009). The structural differences between Gram-negative and positive bacteria are indicated in Figure 1.1. The outer membrane is one of the vital organelles in the bacterial cell which serves as the protective barrier against antibiotics and other toxins (Santajit and Indrawattana, 2016). In addition to facilitating MDR, this membrane also transmits signals from the toxic agents to the bacteria and it facilitates the uptake of nutrients, which are important for the bacteria's survival through the porins (Karlowsky *et al.*, 2017).

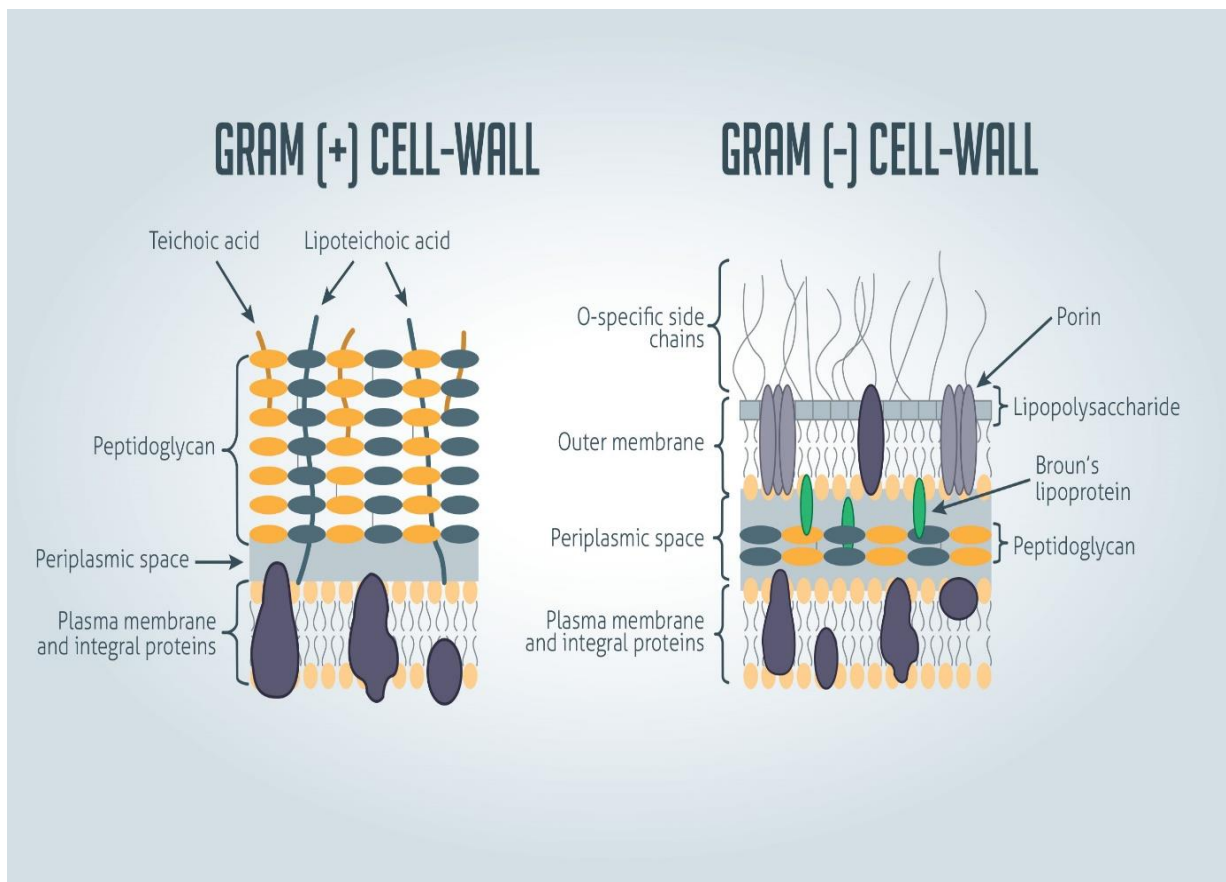


Figure 1.1: Schematic diagram depicting the variance between the outer membrane of Gram-positive and Gram-negative bacteria. The Gram-negative bacteria comprise of a thick outer membrane which is bounded by a lipopolysaccharide layer, the Gram-positive bacteria does not have an outer membrane (Adapted from Steward (2022)).

1.3 BACTERIAL BIOFILM

Gram-negative ESKAPE pathogens commonly live on medical instruments such as catheters and ventilators where they form biofilms. These biofilm organizations enable the bacteria to survive and facilitate the development of multidrug resistance since they work as a biochemical shield that protects the bacteria from antimicrobial drugs. A microbial biofilm are clusters of cells adhered to a surface and confined in a matrix that mainly consists of polysaccharides, proteins and extracellular DNA. By forming biofilms, bacteria become more resistant to stress conditions and host immune responses (Vestby *et al.*, 2020). Pathogenic bacteria can survive harsh external environments by forming biofilms and waiting for hosts that are appropriate for them. Bacterial biofilm often has a decreased growth rate, altered gene expression and elevated extracellular polymeric substances (EPS) production (Prakash *et al.*, 2003). As such, bacteria embedded in the biofilm are resistant to most antibiotics. This resistance is attributed to various factors such as the excretion of EPS that serves as a barrier preventing antibiotics from penetrating. Moreover, bacteria in biofilms are usually slow-growing or non-growth coupled with antimicrobial resistance gene expression (Ruhail and Kataria, 2021).

A biofilm forms through an intricate and dynamic process that includes a primary adherence, formation of a micro-colony, maturation and cell dispersion (Figure 1.2). During the initial attachment, the planktonic bacteria reversibly attach to the surface, following attachment a monolayer is formed which leads to the production of an extracellular matrix. Subsequently, the matrix formation becomes dominated by structural proteins and polysaccharides leading to the formation of micro-colonies which grows significantly. The biofilm then grows rapidly and irreversibly thus forming a mature biofilm (Muhammad *et al.*, 2020).

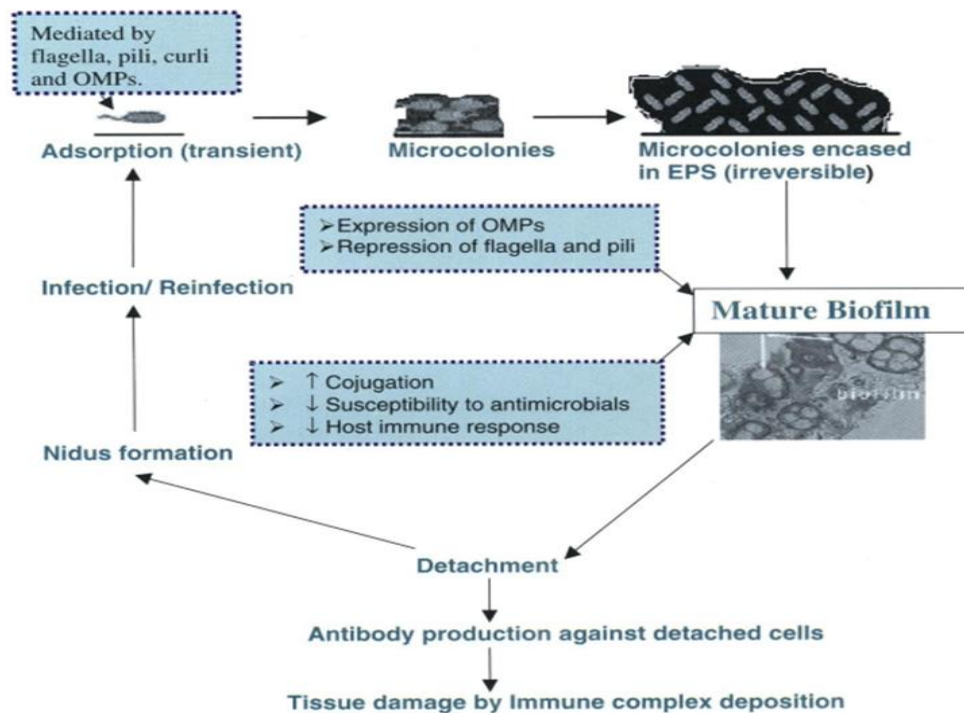


Figure 1.2: Diagrammatic depiction of biofilm formation in microorganisms (Prakash *et al.*, 2003).

Biofilms display different resistance mechanisms as compared to planktonic organisms, such as mutations at target sites, efflux pumps, less permeability of cells and drug modifying enzymes (O’Shaughnessy *et al.*, 2020; Prakash *et al.*, 2003; Ruhali and Kataria, 2021). There are several factors contributing to antibiotic resistance in biofilm communities, such as incomplete or slow diffusion of antimicrobials into the biofilm, subpopulation of microorganisms and reformed chemical microenvironments in the biofilm (Prakash *et al.*, 2003).

In human infections, biofilms are estimated to play a role in 65% of the cases, according to experts at the Centres for Disease Control and Prevention (Vestby *et al.*, 2020). The family of *Enterobacteriaceae* is the major cause of biofilm-associated infections, with the *Enterobacter* species being the prevalent pathogens in most clinical settings (Ruhali and Kataria, 2021). Biofilm is considered a major virulence factor exhibited by pathogens that cause nosocomial infections. It is therefore empirical to understand the process of biofilm formation as well as to find suitable compounds to combat their formation by these pathogens (Ghosh *et al.*, 2020).

1.4 MDR IN ECC

In addition to being the major biofilm-forming species, *Enterobacter* species are resistant to most antibiotics as compared to other ESKAPE pathogens, and they are constantly generating new resistance mechanisms (Karlowsky *et al.*, 2017). *Enterobacter* is a group of Gram-negative bacteria characterized by their rod-shaped shape and usually found in blood and UTIs (Mezzatesta *et al.*, 2012). *Enterobacter* strains that are resistant to the antibiotics class called carbapenems are collectively classified as carbapenem-resistant *Enterobacteriaceae* (CRE) (Wilson *et al.*, 2017). CRE strains are considered the most difficult strains to treat because they are said to be resistant to all available antimicrobial agents, in most cases (Annavajhala *et al.*, 2019). Therefore, CREs are undoubtedly a threat to the healthcare system. According to the data reported by the Veterans' Health Administration (VHA), *Enterobacter cloacae* complex (ECC) are the second most common CRE which genotypically has epidemic potential to spread carbapenem-resistant infections (Wilson *et al.*, 2017). Carbapenem resistance in ECC is due to the gain of carbapenemase genes which are encoded on the plasmid or increased expression of *AmpC* genes (Annavajhala *et al.*, 2019). The main isolates that are part of the *E. cloacae* complex include; *E. cloacae*, *E. kobei*, *E. asburiae*, *E. hormaechei* and *E. xiangfangensis* (Mezzatesta *et al.*, 2012). The ECC pathogens are mostly associated with nosocomial infections as well as other infections including septicaemia, pneumonia and urinary tract infections (Mustafa *et al.*, 2020). The focus on these pathogens is driven by the increased advent of MDR (Mezzatesta *et al.*, 2012).

Penicillin was the first antibiotic that was discovered in 1928, since then many other antibiotics have been produced commercially (Vivas *et al.*, 2019). Antibiotics play a vital role in treating and preventing infections that are caused by bacteria. However, many bacterial strains have become resistant to a variety of antibiotics including methicillin, vancomycin, lipopeptides, macrolides, fluoroquinolones, oxazolidinones, and combinations of β -lactams and β -lactamase inhibitor combinations (Nikaido, 2009). When bacteria, viruses, and fungi no longer respond to antimicrobial drugs meant to kill them, it is known as antimicrobial resistance (AMR). Most bacteria develop resistance to most antibiotics, which makes eradicating bacterial infections difficult (Vivas *et al.*, 2019).

Resistance develops as a result of misuse or overuse of antibiotics. Furthermore, AMR is a biological phenomenon that occurs naturally over time due to genetic changes (Yang *et al.*, 2021). Bacteria may acquire mutations in the target protein which may reduce their susceptibility to the target drug. For instance, resistance to fluoroquinolone is due to mutations that occur in the target DNA topoisomerases or efflux pumps genes (Santajit and Indrawattana, 2016). Multidrug resistance in bacteria may also be due to various mechanisms such as the accumulation of multiple genes in the resistance plasmid (R-plasmid), these genes may code for resistance to a particular antibiotic (Oliveira *et al.*, 2020). Additionally, the overexpression of multidrug efflux pumps coding genes also leads to MDR because each of the efflux pumps can pump out more than one drug molecule and thus drug access to the cell is reduced (Annavajhala *et al.*, 2019). There are five classes of bacterial efflux pumps including the multidrug and toxic compound extrusion (MATE), major facilitator (MF), resistance-nodulation-division (RND), ATP-binding cassette (ABC) and small multidrug resistance (SMR) family (Figure 1.3) (Blanco *et al.*, 2016; Webber and Piddock, 2003). Each of the efflux systems can either be multidrug or drug specific. The multidrug efflux proteins are encoded on constitutively expressed chromosomal genes (Poole, 2007).

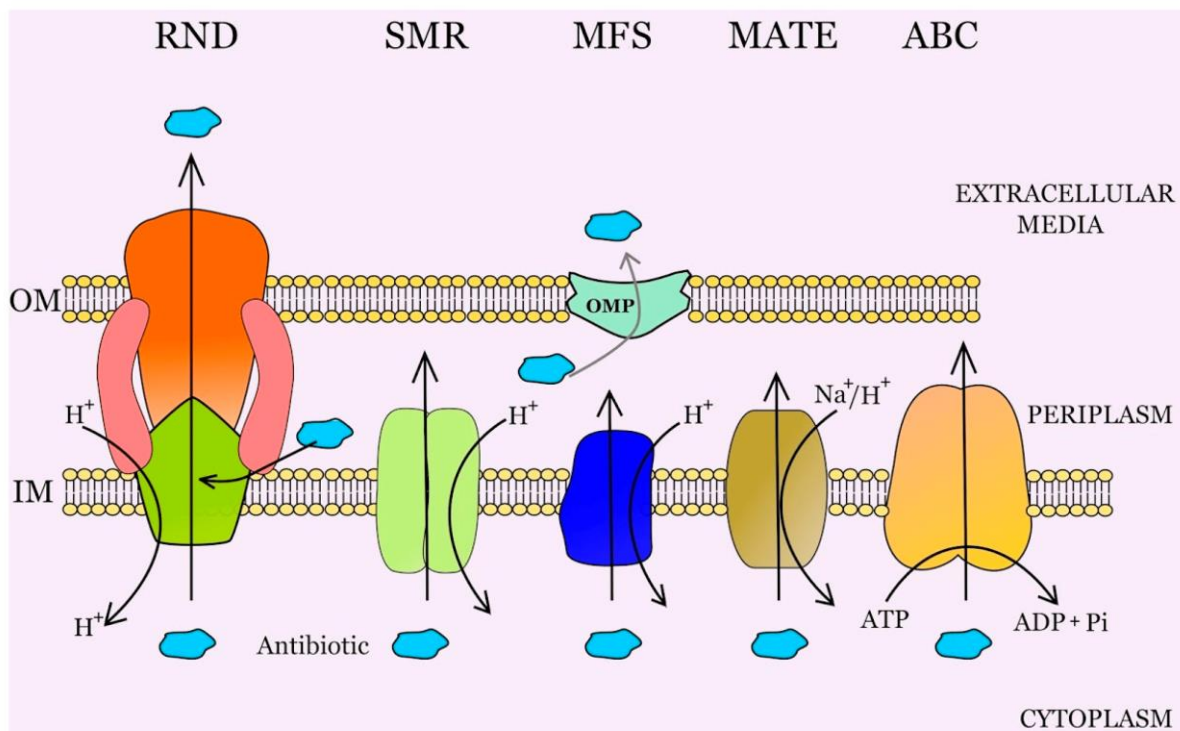


Figure 1.3: Schematic representation of five major efflux pumps family in bacteria (Adapted from Blanco *et al.* (2016))

The low permeability outer membrane as well as the multidrug efflux pumps are associated with enormous resistance mechanisms in Gram-negative bacteria (Karlowsky *et al.*, 2017). As stated above, ECC is one of the most MDR pathogens (Annavajhala *et al.*, 2019). This is because they have plenty of intrinsic and resistance mechanisms which reduces the efficacy of the antimicrobial drugs designed to treat ECC infections (Oliveira *et al.*, 2020). In 1989, the extended-spectrum b-lactamase (ESBL) genes were identified. These genes are encoded in the plasmid of ECC and they give out resistance to b-lactam antibiotics (Mustafa *et al.*, 2020). Moreover, ECC is innately resistant to cephalosporins owing to low levels of *AmpC* genes which code for cephalosporinase (Annavajhala *et al.*, 2019). AMR bacteria can be traced by specific allele profiles. Recent whole genome sequencing (WGS) studies have discovered that nine variable resistance alleles are responsible for the rising trend of AMR (Mustafa *et al.*, 2020).

1.5 USE OF METALS IN MEDICINE

The ideal goal is to formulate antimicrobials that exhibit maximum effectiveness at the lowest possible dose. Most traditional antibiotics are based on targeted therapy, where they target biochemical processes such as transcription, replication, or an enzyme that plays a crucial role in microbial growth (Ma *et al.*, 2020). Despite this, targeted therapy is believed to facilitate the acquisition of resistance relatively easily since bacteria evolve and develop mechanisms that evade the effects of antibiotics (Turner, 2017). Thus, researchers have gained an interest in examining metal-based antimicrobials (MBA) owing to their ability to target multiple biological processes in a cell (Pricker, 1996). MBA were first discovered in the early 20th century prior to the invention of organic antibiotics (Balfourier *et al.*, 2020). Metals have been reported to be able to combat microbial resistance due to their high efficacy against bacteria that form biofilms, one key phenotype which promotes AMR. Most of the metals that have traditionally been considered antibacterial agents are d-block transition metals, such as silver (Ag), gold (Au), cobalt (Co), chromium (Cr) and platinum (Pt) (Pricker, 1996).

1.5.1 GOLD-BASED COMPLEXES

The use of gold in medicine dates to 2500 BC as documented in Chinese medicine. Gold was viewed as a precious drug with many health benefits; however, it was mainly used for treating seizures, palpitations and wounds (Balfourier *et al.*, 2020). Alchemists in ancient Europe also had a gold-containing medicinal mixture known as aurum potabile (Pricker, 1996). In addition, in the 19th century, "muriate of gold and soda" $\text{Na}[\text{AuCl}_4]$ was used as a syphilis treatment. In 1890, Robert Koch, a German bacteriologist discovered that gold cyanide $\text{k}[\text{Au}(\text{CN})_2]$ inhibits the growth of tubercle bacillus (Wang *et al.*, 2012). Following this, gold therapy was used as a treatment for tuberculosis, but ultimately it was found that gold therapy was ineffective with toxicity exceeding the therapeutic advantage (Benedek, 2004). Additionally, within the 20th century, gold complexes were also presented as a treatment for rheumatoid arthritis (Pricker, 1996). Where the early gold molecules utilized were gold (I) thiolates (AuSR) such as solganol and myocrisin, however, the use of these compounds was later prohibited due to their slow activity and severe side effects (Wang *et al.*, 2012). In 1985, auranofin (R_3OAuSR) was introduced as the first oral drug for rheumatoid arthritis (RA). Auranofin is a thiolate monomer with a phosphine ligand that makes it lipophilic (Pricker, 1996). Gold thiol compounds have been shown to undergo ligand exchange reactions with biological ligands including the amino acid cysteine in bacteria (Wang *et al.*, 2016).

In vitro studies have shown that gold phosphine complexes show bactericidal activity against *P. putida*. Moreover, a gold(I) thiocyanate complex was reported to be cytotoxic towards Gram positive bacteria including methicillin-resistant *S. aureus* (MRSA) (Shamaila *et al.*, 2016). Further research on gold compounds resulted in the discovery of gold(I) phosphonium dithiocarboxylate compounds which also have activity against Gram positive bacteria including some cocci (Ortego *et al.*, 2015a). However, studies reporting the antibacterial activity of gold compounds are limited due to stability problems in their formulation (Ratia *et al.*, 2022)

1.5.2 PLATINUM-BASED COMPLEXES

The medicinal properties of platinum-based compounds have also been explored since the discovery of cisplatin (cis- diamminedichloroplatinum (II)) in the 19th century. Cisplatin is a platinum-based drug that is commercially used to treat various cancer tumours such as ovarian, testicular, bladder, colorectal, lung, head and neck cancers (Dilruba and Kalayda, 2016). The chemotherapeutic properties of cisplatin were first unveiled by Barnett Rosenberg in the 1960s while he was investigating how electric field affects bacterial growth (Dilruba and Kalayda, 2016). Furthermore, in 1966 Rosenberg and colleagues reported that platinum (IV) compounds were bacteriostatic against *Escherichia coli*. This further gave insight into the antimicrobial properties of platinum (Oun *et al.*, 2018).

Researchers then began to investigate the antimicrobial abilities of platinum, to develop new antibiotics and combat AMR. In a study conducted by Frei and coworkers (2021), platinum cyclooctadiene (COD) compounds were found to be active against a panel of Gram-positive bacteria, including methicillin- and vancomycin-resistant *S. aureus* (Frei *et al.*, 2021). The COD complexes were mainly selective towards bacteria and exhibited no toxicity to human embryonic kidney cells; however, high serum binding reduced their bioavailability *in vivo* (Frei *et al.*, 2021). In a recent study, numerous metal-based complexes exhibited a 10-fold higher hit-rate against ESKAPE pathogens than the organic molecules studied (Frei *et al.*, 2021). Out of the 906 metal complexes examined, 63 contained platinum. This indicates that platinum-based complexes do not only exhibit anticancer properties but can putatively be used as antimicrobial agents as well (B. Wu *et al.*, 2019).

1.5.3 SILVER-BASED COMPOUNDS

Metal-based antimicrobials have been in existence for over a century. Those derived from silver and copper have had the most commercial success (Alexander, 2009). Silver has been used medicinally since 4000 BC to prevent infections or treat diseases. In the 1800s, silver nitrate (AgNO_3) was used topically to treat burns, ulcerations and infected wounds (Medici *et al.*, 2019). Moreover, AgNO_3 was also used to treat gonococcal ophthalmic infections in neonates (Barillo and Marx, 2014).

However, the advent of antibiotics after World War II resulted in a decline in the use of AgNO₃. Moreover, the use of AgNO₃ in open wounds has been shown to be harmful to human tissue hence its use as an antimicrobial agent is limited (Li *et al.*, 2016). Further studies on revitalizing the use of silver in the form of silver sulfadiazine has led to continuing investigations of silver's topical use to reduce bacterial burden and promote healing in chronic wounds, blood and urinary catheters (Alexander, 2009). Studies have shown that silver-coated urinary catheters combat urinary infections better than alloyed catheters (Politano *et al.*, 2013). In addition, wound dressings that contain Ag were found to be more effective in reducing the viability of bacterial cells by 99% (Alexander, 2009).

Silver has also been shown to significantly reduce the viability of *K. pneumoniae* and *Staphylococcus spp.* Silver metals are therefore, perhaps, a potential weapon against infectious diseases (Morones-Ramirez *et al.*, 2013). However, their bioavailability depends on the solubility, delivery method, ionization, silver sources, and concentration of ligands they bind to such as silver-binding protein (SilE) protein, halide ions and other biological peptides (Politano *et al.*, 2013). Owing to advances in molecular genetics, scientists have been able to gain insight about the mechanisms of silver resistance in bacteria, specifically in *Salmonella* (Silver, 2003). Nine genes were implicated in these transcription units. The periplasmic binding of Ag(I) to proteins SilE and SilP is regulated by a sensor plus a three protein chemiosmotic exchange system and two efflux pumps (Konop *et al.*, 2016).

Ferreira and colleagues (2015) investigated the properties of silver(I) phosphine compounds on different cancer cell lines, and the study found that the compounds selectively induced apoptosis in MCF-7 breast cancer cells. In preliminary findings with selected Gram-negative and Gram-positive bacteria, silver(I) phosphine compounds have also been shown to putatively inhibit bacterial growth, so it was deemed necessary to examine these initial findings in greater details. Moreover, various studies in literature have shown that silver(I) compounds are excellent antimicrobials and thus it is necessary to investigate the antimicrobial properties of these generic compounds as potential antibiotics (Politano *et al.*, 2013)

1.6 HEAVY-METAL RESISTANCE IN *ENTEROBACTER XIANGFANGENSIS* PB204

Apart from antibiotic resistance, bacteria have also evolved the ability to tolerate high levels of heavy metals. Heavy metal resistance is mostly prevalent in bacteria isolated from toxic environments such as mines, industrial waste sites and near volcanoes (Aljerf and AlMasri, 2018). However, heavy metal resistance spreads rapidly due to horizontal gene transfer. Genes encoding heavy metal resistance can be found on the chromosome of the bacteria or on the extrachromosomal elements such as plasmids (Nies, 1999). To date, five main mechanisms by which bacteria resist heavy metals have been reported, including reduced metal ions, extracellular and intracellular sequestration, extracellular barrier and active transport of metal ions via efflux pumps (Ianeva, 2009). Numerous studies have indicated a positive correlation between antibiotic resistance and heavy metal resistance. Locations contaminated with metals tend to harbour an abundance of antibiotic resistant bacteria, and genes conferring co-selection to heavy metals and antimicrobials are habitually acquired concurrently in most clinical settings (Baker-Austin et al., 2006). Furthermore, researchers have found that genes associated with metal and antibiotic resistance are frequently clustered within the same element, especially on the plasmid, leading to the co-selection of other genes within the element (Aljerf and AlMasri, 2018).

A co-selection of heavy metal resistance genes (*merA*, *arsA*, *pcoA* and *silC*) have been found Enterobacteriaceae carrying the antibiotic resistant genes $[\text{bla}]_{\text{NDM-1}}$ and $[\text{bla}]_{\text{CTX-M-15}}$ (Yang et al., 2018). Various mechanisms which facilitate the co-selection of antibiotic and metal resistance have been elucidated. Co-resistance and cross-resistance are part of the proposed mechanisms for co-selection (Baker-Austin et al., 2006). Several studies have provided evidence for co-resistance though plasmid sequencing together with phenotypic and bioinformatic analysis, it has been shown that most plasmids contain genes which encode metal and antibiotic resistance (Yang et al., 2018). Antimicrobial agent cross-resistance occurs when agents target the same biological pathway or share a common mechanism leading to microbial death or access to the cell. This phenomenon occurs when structurally dissimilar compounds are emitted using the same mechanism (Baker-Austin et al., 2006).

Herein, the susceptibility or resistance of *E. xiangfangensis* to various silver(I) phosphine complexes was investigated. *Enterobacter xiangfangensis* is a Gram-negative, facultative anaerobic bacterium (Mustafa *et al.*, 2020). This strain grows in circular, smooth, convex, white colonies after 24 hours of incubation at 30°C on nutrient agar. The type strain *E. xiangfangensis* LMG 27195^T was first isolated from a traditional Chinese sourdough in the *Xiangfang* district (Gu *et al.*, 2014). Recent studies have shown that *E. xiangfangensis* is the most dominant *Enterobacter* species which causes nosocomial infections rather than *Enterobacter cloacae* (Liu *et al.*, 2013). A metal resistant strain *E. xiangfangensis* Pb204 was isolated from an acid mine discharge in a uranium mine in South Africa (Ho *et al.*, 2018b). This bacterium has a propensity to produce gold nanoparticles. Gold nanoparticles are important in biomedicine and biotechnology (Shamaila *et al.*, 2016). The genome of *E. xiangfangensis* Pb204 is bigger than *E. xiangfangensis* LMG 27195^T due to the presence of the ICE element shown in Figure 1.4 (Ho *et al.*, 2018b). ICE elements are “self-transmissible” integrative elements found in various Gram-negative and positive bacteria (De Maayer *et al.*, 2015). These elements accumulate through the horizontal exchange of genetic elements, and they have an impact on the bacteria’s ability to adapt to new environments (Nikaido, 2009). ICE_{xi}Pb204 codes for 28 proteins involved in arsenic, zinc, silver, and copper resistance pathway (Ho *et al.*, 2018b).

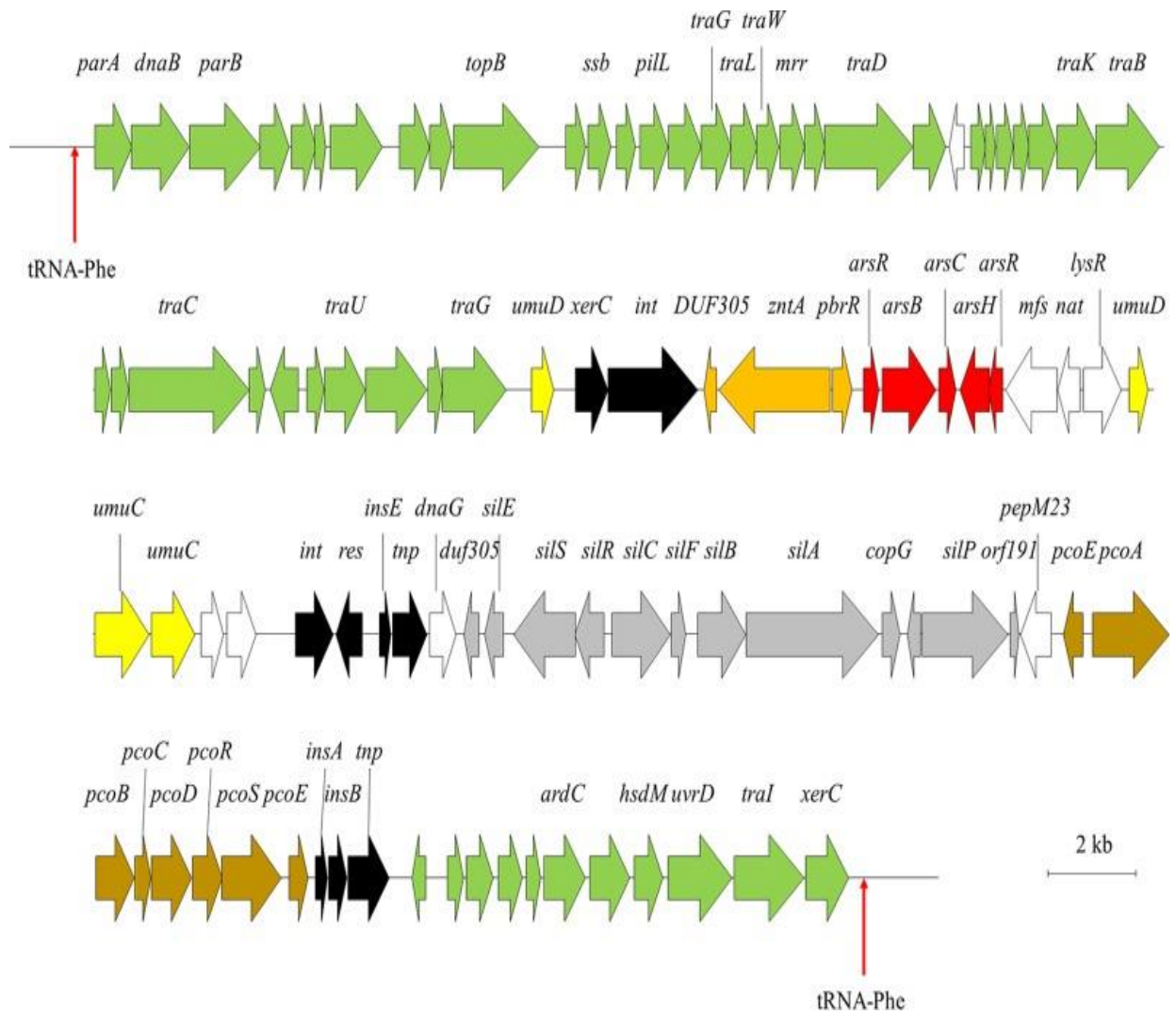


Figure 1.4: Schematic diagram of ICEXiPb204. The genes for the silver, gold, zinc, arsenic and copper resistance pathways are shown. Green arrows signify the integration, excision, and maintenance of ICE-related proteins. Yellow arrows denote genes involved in DNA damage SOS response (umuDC). Transposons and genes coding for hypothetical proteins are shown in black and white (Adapted from Ho *et al.*, (2018))

1.7 AIMS AND OBJECTIVES.

Nosocomial infections are infections that are often acquired in hospitals due to prolonged stay. The emergence of antimicrobial resistance in bacteria, especially the ESKAPE pathogens makes it difficult to eradicate these infections. Recent studies have shown that *E. xiangfangensis* is the main clinical culprit in the *E. cloacae* complex, thus making it the main target among the ESKAPE pathogens. Owing to their ability to target multiple biological processes in a cell, metal-based antimicrobials have shown promising effect against microbes and thus silver(I) phosphine compounds could be of great potential.

Therefore, the aims of the study were to:

1. Investigate the antibacterial and antibiofilm properties of novel silver(I) phosphine compounds against the ESKAPE pathogens.
2. Assess the mechanisms of silver resistance of *E. xiangfangensis* Pb204 through gene expression and whole genome analysis.

To achieve these aims, the following objectives were addressed:

- Screening the bacteria for susceptibility or resistance to various silver(I) phosphines using the minimum inhibitory concentration (MIC) microdilution technique.
- Evaluating the effect of the silver(I) phosphine compounds on biofilm formation and degradation using an optimised antibiofilm assay with crystal violet.
- Determining the effect of the silver(I) phosphine compounds on the metabolic activity of cells in biofilms using XTT assay.
- *In-silico* design of primers for the genes coding for proteins involved in the silver resistance pathway of *E. xiangfangensis* Pb204.
- Quantifying the expression of genes involved in the silver resistance pathway (*silA*, *silS* and *silR*) using RT-qPCR.
- Comparative genomics using Orthofinder to identify core and unique proteins between *E. xiangfangensis* Pb204 and *E. xiangfangensis* LMG 27195^T.
- To classify functionally distinct orthogroups according to their non-supervised orthologous groups (NOGs) using eggNOG mapper.

CHAPTER TWO: METHODS AND MATERIALS

2.1 MEDIA AND AGAR PREPARATION

Luria-Bertani (LB) broth (NEOGEN, USA) was prepared in a 1 L bottle, where 25 g of medium was dissolved in 1 L distilled water and mixed thoroughly. The LB mixture was then autoclaved at 121 °C for 30 min and stored at 4 °C. For plate streaking purposes, LB agar was made by dissolving 15 g of Bacto™ agar (Difco, France), 25 g of LB broth (NEOGEN, USA) in 1 L distilled water. The mixture was autoclaved to sterilize and melt the agar completely. After autoclaving, the LB agar mixture was set to cool down and then it was poured into Petri-dishes (25 mL) and the agar was allowed to solidify (all work was done under a sterile laminar flow).

2.2 BACTERIA CULTURING

The *E. xiangfangensis* LMG 27195^T strain was purchased as a freeze-dried culture from Belgian coordinated collections of microorganisms (BCCM), and the *E. xiangfangensis* Pb204 strain was kindly provided by Prof Kulsum (University of Johannesburg). The microorganisms were grown on LB media (NEOGEN, USA). Both strains were first streaked on an agar plate then a single colony was isolated from each agar plate and transferred into 30 mL of LB media after which the inoculum was incubated for 24 h at 37 °C. After incubation, the established cultures (1 mL) were sub-cultured into fresh broth (10 mL). In order to maintain the logarithmic growth phase of the microorganisms, the cultures were sub-cultured daily.

2.3 PREPARATION OF COMPOUNDS

In this study, eight different silver(I) phosphine compounds were investigated namely, UJ1, UJ2, UJ3, UJ4, UJ1A, UJ15, UJ34 and UJ35. The compounds were chemically synthesized at the University of Johannesburg in the Department of Chemical Sciences. All compounds were validated by chemical analyses and the chemical structures are included in Appendix A. For treatment purposes, a 1 mg/mL stock solution of each compound was made by dissolving 1 mg of the respective compounds in 1 mL dimethyl sulfoxide (DMSO) solvent (ACE, SA). The solutions were heated at 70 °C for 1 h to solubilize them, and then they were stored in the dark. Before each experiment, the compounds were pre-heated at 70 °C for 45 min to ensure they were fully dissolved before being used.

2.4 MINIMUM INHIBITORY CONCENTRATION (MIC) ASSAY

The ability of an antimicrobial agent to hinder microbial growth can be assessed through different techniques, including but not limited to fluorimetry, turbidity measurement, bioluminescence, viability and direct microscopic counts (Balouiri *et al.*, 2016; Gajic *et al.*, 2022). The agar diffusion method is the most practised assay to assess antimicrobial activity. The results obtained with agar diffusion assays are influenced by various factors such as the agar type used, incubation time, salt concentration and molecular size of the antimicrobial agent (Bonev *et al.*, 2008). While this technique is effective for well-defined antimicrobials, its use is limited when novel antimicrobial agents are used (Balouiri *et al.*, 2016). Moreover, the minimum MIC of the antimicrobial agent cannot be established through the agar diffusion assay. Hence, when the MIC of an agent needs to be determined, the Clinical and Laboratory Standards Institute (CLSI) recommends either the micro broth or microdilution methods (Gajic *et al.*, 2022). In the microdilution method, microtiter plates are utilised which enables many samples to be analysed in a short period. Tetrazolium salts are utilized as indicators of biological activity where live bacteria can convert formazan to a coloured product that can be easily assessed (Eloff, 1998; Klančnik *et al.*, 2010).

A MIC assay was done on a 96-well plate using a microdilution method. The treatments were prepared, before bacterial cell addition, 100 μL of a 1 mg/mL stock of the silver(I) phosphine compound was added in the first set of wells in triplicate. The starting concentration was serially diluted five times by adding 100 μL LB broth such that the final volume of treatment in each well was 100 μL . Figure 2.1 shows the treatments that were added to each well and their respective concentrations following the serial dilution of the compounds. The treatment for each tested compound was done in triplicate. Following the serial dilution of the compounds, 100 μL of the diluted bacteria ($A_{600} \approx 0.06$) was added to each well, except for the wells containing media only, making up 200 μL per well. To determine if the solvent/vehicle control, DMSO, had any effect on the bacterial cell growth, cells were incubated with 25% DMSO which is the highest concentration included in the stock solutions of the complexes. In addition, a negative control, consisting of 200 μL of LB media only, was also included as well as 200 μL untreated control. Moreover, two silver salts, silver nitrate (AgNO_3) (Sigma-Aldrich, USA) and silver sulfadiazine (AgSD) (Acros Organics, China), serving as positive antimicrobial controls, were also included as treatments. The fully prepared

96-well plate was then incubated for 24 h at 37°C. After incubation, 30 µL of 2 mg/ml Iodotetrazolium chloride (INT) dye (Sigma-Aldrich, Germany) was added to all the wells and the plate was further incubated for 1 h at 37 °C to observe a colour change. The INT dye (Sigma-Aldrich, Germany) was used to indicate the inhibition of cellular growth. The bactericidal or bacteriostatic effects of the compounds were determined by monitoring the cellular recovery of the treated bacterial cells of which inhibition was noted. To do this, 20 µL of the bacterial cell suspension that remained clear (no colour change on the well), including the untreated and vehicle controls, were spread on individual agar plates and incubated at 37 °C. These plates were then monitored for recovery or bacterial cell growth for a period of 48 h.



Figure 2.1: Template illustrating how the 96-well plates were prepared and the concentration range used for minimum inhibitory concentration studies for the broth dilution method. Serial dilutions of the compounds (silver(I) or positive controls silver nitrate and silver sulfadiazine) were done on the *Enterobacter xiangfangensis* pathogens. In addition, a positive untreated, negative media control and vehicle control, 25% (w/v) DMSO was also included. A total of eight different silver (I) phosphine compounds were tested, and 4 compounds were serially diluted in one plate (the colours on the plate indicate different treatments: UJ1, UJ2, UJ3, UJ4).

2.5 ANTIBIOFILM ASSAY

Biofilm formation is the process whereby microorganisms adhere to the surfaces and form clusters (Vestby *et al.*, 2020). Upon attachment of the planktonic cells to the surface, the EPS and additional layers of microbes are established within a few hours and are known as immature biofilms. In 12 h the biofilm evolves and matures, burying the bacteria further into the matrix which makes it more resistant to antimicrobial agents and causing it to become a mature biofilm (Chandki *et al.*, 2011; Fu *et al.*, 2021). To investigate the formation of biofilms two distinct techniques are normally used, either a static or dynamic approach. In a dynamic setup, mature biofilms can be established (Kishen and Haapasalo, 2010). However, these setups require specialized continuous-flow equipment such as biofilm reactors. Owing to its flexibility, feasibility, high throughput and low cost, the static approach is the most used method to study biofilm formation (Wilson *et al.*, 2017). This approach does not allow for the formation of mature biofilms; therefore, it is often used to evaluate the early stages of biofilm formation (Kishen and Haapasalo, 2010). The crystal violet (CV) based assay is the most common method used to study the early stages of bacterial biofilm formation. In this method, a polystyrene microtiter plate is used where the biofilm forms on the wall or on the bottom of a microtiter plate hence it is efficient in testing biofilm formation by multiple strains under various conditions (Kishen and Haapasalo, 2010; Song *et al.*, 2019; Xu *et al.*, 2016).

2.5.1 ESTABLISHING A BIOFILM

The bacterial cultures of the *E. xiangfangensis* Pb204 and *E. xiangfangensis* LMG 27195^T were grown overnight in LB medium as described in section 2.1. The overnight cultures were diluted ($A_{600} \approx 0.06$) into fresh LB medium for the biofilm assays. To assess the effect of the compound on biofilm formation, 100 μ L diluted cell suspensions were added in each well along (co-incubated) with 50 μ L of the various silver(I) phosphine compounds using the MIC concentrations (Table 3.1) to make the final volume of 200 μ L. For the untreated control, 200 μ L of cell suspension was added on the well. The plates were then incubated at 37 °C for 48 h with shaking at 120 rpm for biofilm formation. To investigate whether the compounds can disrupt or degrade the biofilms formed by the two strains, biofilms were allowed to form without any treatment. According to Gemba and coworkers (2022), *E. xiangfangensis* (formerly known as *E. hormaechei*) forms strong matured biofilm after 48 h incubation at 37 °C.

The biofilms were formed following the protocol by Gemba and coworkers (2022) with few modifications. Briefly, 200 μ L of the cell suspension was added into a 96-well plate in triplicate then the plate was incubated at 37 °C for 48 h at 120 rpm. Following 48 h biofilm formation, unattached cells were washed with 200 μ L cold PBS(0.1 g KCl, 0.72 g Na₂HPO₄, 0.1125 g KH₂PO₄, 4 g NaCl, 497,5 ml distilled water). The 48 h formed biofilms were either treated with the MIC concentrations (20 μ L) of the silver phosphine compounds or the two positive control silver salts followed by incubation at 37 °C for 24 h with shaking at 120 rpm.

2.5.2 MICROTITER DISH BIOFILM FORMATION ASSAY

2.5.2.1 CRYSTAL VIOLET ASSAY

After 48 h of biofilm formation, the supernatants in each well were discarded and the wells were washed twice with 200 μ L of cold PBS to remove unattached cells. The plate was then air-dried in the biohazard cabinet for 30 min to allow the biofilm to dry completely. Subsequently, 100 μ L of 0.5% (v/v) crystal violet solution was added to each well then, the plate was incubated at 37 °C for 1 h. After incubation, the reserve crystal violet was discarded, and each well was washed twice using 200 μ L Milli-Q water. Thereafter, 200 μ L of 95% (v/v) alcohol was added to de-stain the attached cells for 45 min at room temperature. In a new plate, 100 μ L of the destaining solution was added and the amount of crystal violet was measured using a VICTOR Nivo[®] Multimode plate reader (PerkinElmer, UK) at an absorbance of 595 nm. To eliminate background interference, the absorbance readings of the negative controls (wells containing sterile LB medium) were deducted from the test wells. The assay was repeated three times for each bacterial strain.

2.5.2.2 XTT ASSAY

Following the formation of biofilms, the wells were washed twice with 200 μ L of PBS and the XTT assay was done using the CyQUANT™ XTT kit (Thermo Fisher Scientific, USA) as per manufacturer's instructions. For the XTT-menadione stock solution (freshly prepared for each set of assays on the day) 1.5 ml of XTT (1 mg/mL in sterile saline) was added to 300 μ L menadione solution. Thereafter, 15 μ L of XTT-menadione stock solution was added to each well along with 200 μ L of PBS followed by incubation for 2 h at 37°C in the dark. After incubation, 100 μ L XTT solution was transferred to a

new well and the absorbance was quantified at 490 nm and 660 nm using a VICTOR Nivo® Multimode plate reader (PerkinElmer, UK).

2.6 QUANTITATIVE REVERSE TRANSCRIPTION PCR

Quantitative reverse transcription PCR (RT-qPCR), also known as real-time PCR, is a technique that is used to quantify the copy number of PCR templates such as complementary DNA (cDNA) or DNA (Denman and McSweeney, 2005). RT-qPCR is often used in gene expression studies, genetic testing and microarray detection. In conventional PCR, the PCR amplicon is detected at the endpoint whereas in RT-qPCR the amplification product is measured in real time as the reaction progresses (Kralik and Ricchi, 2017). The real-time detection of the amplicon is due to the presence of a fluorescent reporter molecule used in each reaction (Arya *et al.*, 2005). The amount of quantified fluorescence is directly proportional to the total amount of amplicon thus the change in fluorescence over time is used to determine the amount of amplicon produced in each cycle (Denman and McSweeney, 2005; Kralik and Ricchi, 2017).

When RT-qPCR is conducted, RNA is used as a starting material which is obtained after extraction. The purity of RNA is evaluated by measuring the 260/230 nm and 260/280 nm ratio using a spectrophotometer, where high absorbance at 230 nm dictates the presence of phenol in the sample and high absorbance at 280 nm may indicate protein contamination in the sample (Denman and McSweeney, 2005). The integrity of RNA is also validated to make sure that there is no genomic DNA (gDNA) contamination which can produce a false positive during RT-PCR, this is normally done using agarose gel electrophoresis. Once the purity of the RNA is assessed, the RNA can be transcribed into cDNA by reverse transcriptase (Bonev *et al.*, 2008; Denman and McSweeney, 2005; Kralik and Ricchi, 2017).

2.6.1 RNA ISOLATION

2.6.1.1 LYSATE PREPARATION FROM BACTERIA

Unlike most eukaryotic cells, bacterial cells are protected by cell walls which can be arduous to destroy (Ares, 2012). Therefore, effective cell lysis through mechanical disruption (bead homogenizer) or enzymatic treatment (glycinate or lysozyme) is required before RNA is extracted from bacterial cells (Primo *et al.*, 2018). To prepare a bacterial lysate for extraction, the bacterial cell culture (OD = 0.2) was first incubated

with the selected treatments (UJ1, AgSD, AgNO₃ and Untreated control was included) at ½ MIC (Table 3.1) for 16 h at 37 °C. After 16 h incubation, the treated cultures were centrifuged at 13 500 x g for 15 min to separate the cells from the media. The supernatant was disposed, and the remaining media was removed by aspiration. The cells were then washed with 25 ml of ice-cold 1XPBS and centrifuged at 300 x g for 5 min. Following centrifugation, the supernatant was discarded, and the bacteria pellet was resuspended in 100 µL of lysozyme-containing TE buffer (1 mg/mL). In order to lyse the cell walls of the bacteria, the cells were incubated for 5 min at room temperature. After incubation, the lysate was transferred into a sterile 1.5 ml tube and 350 µL RNA dilution buffer from the Promega SV Total RNA Isolation System kit (Promega, USA) was added. The mixture was placed in a heating block at 70 °C for 3 min and then centrifuged at 13 500 x g for 10 min at 25 °C.

This was followed by purifying the RNA using the SV Total RNA Isolation System (Promega, USA) as per the manufacturer's instructions. Briefly, the lysate solution prepared in 2.6.1.1 was transferred into fresh microcentrifuge tubes by transferring the supernatant to a new tube and the pellet was discarded. Thereafter, 200 µL of 95% ethanol was added to the supernatant and agitated. This was then transferred into a spin column assembly and centrifuged for 1 min at 13 500 x g. In a spin column assembly, 600 µL of RNA Wash Solution was added followed by DNA elimination. For this, a DNA incubation mix was prepared by adding 40 µL yellow core buffer, 5 µL 0.09M MnCl₂ and 5 µL of DNase I in a sterile tube. The DNA incubation mix (50 µL) was added to the spin column and incubated for 15 min at 25 °C followed by the addition of 200 µL of DNase Stop Solution and centrifuged for 1 min at 13 500 x g. This was again followed by washing using 600 µL of the RNA wash solution and centrifugation for 1 min at 13500 x g. The collection tube was emptied and 250 µL RNA Wash Solution was added to the column then centrifuged for 2 min at 13 500 x g. The spin column was then transferred to an elution tube where 100 µL nuclease free water was added. Finally, the total RNA was then eluted by centrifuging the tube for 1 min at 13 500 x g.

2.6.1.2 RNA QUANTITY AND INTEGRITY

The NANODROP ONE (Thermo scientific, USA) spectrophotometer was used to quantify and determine the quality of the extracted RNA. This was done by measuring 1 μ L of the extracted RNA samples on the nanodrop pedestal. The samples with 260/230 nm ratio between 2-2.2 and 260/280 nm ratio between 1.8-2.1 were considered pure and were selected. To assess the integrity of the RNA, the selected extracted RNA samples were run on a 1% (w/v) agarose gel (0.5 g of agarose powder and 50 ml 1 X TAE buffer). The agarose solution was heated in the microwave for the agarose to completely dissolve in the TAE buffer. After being dissolved, 1 μ L of ethidium bromide (Sigma-Aldrich, Germany) was added to the solution and swirled gently. The agarose solution was then decanted into the casting tray and left for 30 min to solidify. The solidified gel was positioned in an agarose gel system along with 1 X TAE buffer. The total RNA (1 μ g) of each treatment with the volume calculated using the Nanodrop readings of the RNA concentration were loaded along with 1/6 volume of Blue/Orange 6X Loading Dye (Fermentas) into the wells and resolved at 100 V for 45 min using the Mini-Sub™ cell GT (Bio-Rad, Italy) and PowerPac™ power supply (Bio-Rad, Singapore) agarose gel system. The integrity of the 16S RNA subunit was visualized using a Gel Doc View system (Bio-Rad, USA). After assessing the purity and integrity of the extracted RNA, it was then converted into cDNA on the same day of extraction.

2.6.2 CDNA SYNTHESIS

The cDNA was synthesized using iScript cDNA Synthesis (Bio-Rad, USA) as per the manufacturer's instructions. For each reaction, 4 μ L 5x iScript Reaction mix, 1 μ L iScript reverse transcriptase, and 1 μ g total RNA (the volume was calculated as per concentration of RNA per sample) were added into a PCR tube and equalled to a final volume of 20 μ L. The prepared mixture was then incubated in a Bio-Rad T100™ thermal cycler with the following conditions: 5 min at 25 °C (priming), 20 min at 46 °C (reverse transcription), 1 min at 95 °C (RT inactivation) and a lastly 4 °C for 2 min (hold). The synthesized cDNA was quantified using a NANODROP ONE (Thermo scientific, USA) spectrophotometer and the integrity was assessed by using agarose gel electrophoresis (as described in section 2.6.1.2). The cDNA was then stored at -20 °C for later use.

2.6.3 PRIMER DESIGN

The primers for the *silA*, *silR* and *silS* genes (genes coding for silver resistance pathway) were designed using the IDT PrimerQuest™ Tool (Table 2.1). Subsequently, the Basic Local Alignment Tool (BLAST) was utilized to verify if the primer sequences bind or align to the genome of the species of interest (*E. xiangfangensis* Pb204). The designed oligonucleotide sequences were synthesized at Inqaba Biotec (South Africa).

Table 2.1: Primer sequences for specific genes coding for the silver resistance pathway as well as the housekeeping gene (*gyrB*)

Gene	Forward primer sequence	Reverse primer sequence	Tm	GC Percent
<i>gyrB</i>	AGTACAACCCGGAC AAACTG	GGCATCTGACGATAGAAG AAGG	62	50
<i>silA</i>	CCGAAATGAGGCGT GGTATT	CCTTCAGCGTCTCCAGTTT ATC	62	50
<i>silR</i>	CCATGACAGCCGAG TATGATTTA	GTAAGACCGGCATACCCTT TC	62	52.3
<i>silS</i>	TTATCGCCTTCACCT GGTTTAT	GTTCAGTGTGGTGCTGATT TG	62	47.6

2.6.4 QUANTITATIVE REAL-TIME PCR

RT-qPCR was done using the iTaq Universal SYBR® Green (Bio-Rad, USA) two-step kit in order to measure the level of gene expression, the manufacturer's instructions were followed. The assay master mix for the reactions was prepared by adding 10 µL iTaq Universal SYBR Green super mix, 0.1 µL forward and reverse primers, 100 ng cDNA template and nuclease-free water to make 20 µL total reaction mix volume. The CFX96™ Real-time System (Bio-Rad, Singapore) was used, and the thermal cycling protocol was programmed with the following settings: Polymerase activation and DNA denaturation at 95 °C for 30 seconds, denaturation at 95 °C, annealing and plate reading at 60 °C for 30 sec, 35 cycles and finally melt-curve analysis at 95 °C. The g CFX Maestro (BioRad) was used to analyse the output gene expression. The $\Delta\Delta C_t$

method was used to calculate the level of gene expression, where the housekeeping gene (*gyrB*) was used for normalization.

2.7 COMPARATIVE GENOMICS

2.7.1 COMPARATIVE GENOMICS ANALYSIS

Comparative genomics refers to the field of biology where the complete genomes of different species are compared in order to get an insight about the relatedness of the species as well as the functions of the genes encoded on the genomes (Sivashankari and Shanmughavel, 2007). Through this analysis, the variation and the resemblance between the genomes of the compared species can be elucidated.

Comparative genome analysis was done between the two genomes in order to identify unique and similar genomic features between the two strains. Firstly, the complete genomes of *E. xiangfangensis* Pb204 (GeneBank accession number: CP030007) and *E. xiangfangensis* LMG (GeneBank accession number: CP017183) were obtained from the NCBI genome database. The complete genomes were first visually compared using CGView (Proksee) which is a comparative genomics Java tool which is often utilized to visualize conservation among genome sequences. Proksee uses BLAST to compare the genome sequences and the average nucleotide identity between the genomes is compared through FastANI. Subsequently, the two genomes were functionally and structurally annotated (protein prediction) using the RAST server (Rapid Annotation using Subsystems Technologies). RAST is an automated tool which is often utilized in the annotation of bacterial genomes (Aziz *et al.*, 2008; Brettin *et al.*, 2015; Overbeek *et al.*, 2014). The output predicted protein dataset retrieved from RAST for each strain was then compared using OrthoFinder (v2.3.11) to identify core and unique proteins between the two strains. Orthofinder is a most widely used command-line tool for comparative genomics. It carries out orthology analysis by assuming orthogroups between several species (Emms and Kelly, 2019). After running orthofinder analysis on the command line, the orthogroup dataset was obtained.

Using eggNOG mapper (v2), the unique orthogroup datasets of each genome were then functionally categorized in accordance with their non-supervised orthologous groups. EggNOG mapper is a tool for functional annotation of huge datasets of sequences based on quick orthology assignments utilizing precomputed clusters and phylogenies from the eggNOG dataset (Cantalapiedra *et al.*, 2021) .

2.8 STATISTICAL ANALYSIS

Qualitative and quantitative data was obtained through the MIC assay and cellular recovery monitoring, each of these procedures were done in triplicates. Quantitative data was obtained through RT-qPCR, crystal violet and XTT biofilm assays. For real time qPCR, each sample had n value of 6, two replicates were done per cycles and the experiment was repeated three times. Data from crystal violet and XTT biofilm assay had an n value of nine, where three replicates were done per experiment and each experiment was repeated 3 times. The bar charts were used to represent mean values per sample, with error bars showing the calculated SEM (Standard Error of Mean). The statistical significance of all quantitative data was analysed by means of the student's t-test, where p-values less than 0.001 and 0.01 were considered statistically significant. The comparative genomics was done purely *in-silico* using various bioinformatics tools (online server and on Linux command-line).

CHAPTER THREE: RESULTS

3.1 SCREENING THE ANTIMICROBIAL ACTIVITY OF THE SILVER(I) PHOSPHINE COMPOUNDS

3.1.1 MINIMUM INHIBITORY CONCENTRATION (MIC)

To screen the antimicrobial activity of a compound, it is imperative to utilise an *in vitro* antibacterial assay that is sensitive, easy and reliable. Antibiotic Susceptibility Testing (AST) evaluates how likely it is that a particular antimicrobial agent will inhibit bacterial or fungal growth (Reller *et al.*, 2009). Susceptibility refers to the fact that antimicrobial drugs can inhibit bacterial growth. Therefore, AST is often used to determine if bacteria have developed resistance to antimicrobial drugs or to determine their efficacy in studies or clinical laboratories (Khan *et al.*, 2019). An antibiogram is created from the overall AST results, which helps determine which bacteria exhibit susceptibility/resistance to a particular drug or which drugs are most effective in treating a particular infection (Gajic *et al.*, 2022; Khan *et al.*, 2019; Reller *et al.*, 2009). AST can be performed using phenotypic-based methods, including broth dilution, diffusion, and automated tools. Various genotype-based approaches are also employed in AST, including PCR and DNA microarrays (Reller *et al.*, 2009).

Preliminary studies done in our research group have found that the chemically synthesized novel silver(I) phosphine complexes exhibit antimicrobial properties against the previously studied Gram-negative (*Pseudomonas aeruginosa*), and Gram-positive (*Enterococcus faecalis*) bacterial species. Given this, the antimicrobial activity of eight different silver(I)phosphine compounds were investigated against the ESKAPE pathogen *E. xiangfangensis* Pb204. The susceptibility of *E. xiangfangensis* Pb204 was compared to *E. xiangfangensis* LMG 27195^T.

The AST screening was done using the microtiter technique with INT dye. DMSO was included as a vehicle control to ensure that it does not have an antibacterial effect on *E. xiangfangensis*. This is because 15%(v/v) DMSO has been reported to have inhibitory effect against *B. megaterium*, *E. coli* and *P. aeruginosa* (Ansel *et al.*, 1969). Furthermore, these bacterial strains were also treated with antimicrobial agents (AgNO₃ and AgSD) that are currently being used in wound healing and are referred to

the positive antimicrobial controls (Oaks and Cindass, 2023; Randall *et al.*, 2015). Their effectiveness was compared to that of the silver(I) phosphine compounds using an INT dye. The principle behind the INT dye is that the viable bacteria reduce the yellow dye to pink. However, when bacterial growth is inhibited, the dye is not reduced, and it remains colourless (Eloff, 1999). The MIC values for all the silver(I) complexes including the two controls are presented in Table 3.1. The vehicle control DMSO (25%) did not inhibit the growth of both *E. xiangfangensis* Pb204 and *E. xiangfangensis* LMG 27195^T.

All the silver(I) phosphine compounds tested MIC values were the same at 0.125 mg/ml for both tested strains. When treated with AgNO₃ and AgSD the MIC for *E. xiangfangensis* LMG 27195^T strain was 0.0156 mg/ml for both treatments. However, the observed MIC for AgNO₃ and AgSD for *E. xiangfangensis* Pb204 was 0.03125 and 0.0625 mg/ml, respectively. This shows that *E. xiangfangensis* Pb204 is less susceptible to the silver salts (AgSD and AgNO₃) as compared to *E. xiangfangensis* LMG 27195^T.

Table 3.1: The minimum inhibitory concentration (MIC) of eight various silver(I) phosphine compounds, silver nitrate and silver sulfadiazine (positive control antimicrobial controls) against *Enterobacter xiangfangensis* Pb204 and *Enterobacter xiangfangensis* LMG 27195^T.

	<i>MIC (mg/ml)</i>	
	<i>E.xiangfangensis</i> 27195 ^T	<i>E. xiangfangensis</i> Pb204
AgNO₃	0.0156	0.03125
AgSD	0.0156	0.0625
UJ1	0.125	0.125
UJ2	0.125	0.125
UJ3	0.125	0.125
UJ4	0.125	0.125
UJ1A	0.125	0.125
UJ15	0.125	0.125
UJ34	0.125	0.125
UJ35	0.125	0.125

3.1.2 MINIMUM BACTERICIDAL CONCENTRATION (MBC)

While the MIC studies (Table 3.1) indicate bacterial inhibition at that concentration, it does not necessarily imply complete bacterial eradication. Therefore, the treated bacteria are reintroduced onto a new agar plate to monitor their recovery and to determine the Minimum Bactericidal Concentration (MBC) (Teh *et al.*, 2017). By definition, the MBC is the lowermost concentration of an antimicrobial agent required to kill a bacteria over a fixed or prolonged period (Kowalska-Krochmal and Dudek-Wicher, 2021; Pankey and Sabath, 2004). This was done by reintroducing 20 μ L of the treated bacterial suspension from the MIC test plates (the wells that did not show any colour change) onto a new agar plate followed by incubation at 37 °C. The plates were monitored for growth over a period of 24 h. The concentration where the sample treatment had no cellular recovery (no visible colonies) within the monitored time frame were considered as the MBC (Table 3.2).

The *E. xiangfangensis* Pb204 strain completely recovered after 24 h for all silver(I) phosphine complexes which implies that the MBC exceeds 1 mg/ml. However, the cells treated with AgNO₃ and AgSD did not recover at the concentration of 0.25 mg/ml for both treatments. Interestingly, the *E. xiangfangensis* LMG 27195^T strain showed no signs of recovery when treated with UJ1 with an MBC of 0.25 mg/ml. In contrast, the same bacterial strain recovered when treated with the rest of the silver(I) phosphines. It was also noted that the MBC of *E. xiangfangensis* LMG 27195^T cells when treated with AgNO₃ and AgSD silver salts was lower than the MBC for *E. xiangfangensis* Pb204 cells when treated with the same silver salts (Table 3.2). Based on the findings from the MIC and MBC studies it's evident that *E. xiangfangensis* LMG 27195^T is more susceptible to the UJ1, AgSD and AgNO₃ treatments when compared to *E. xiangfangensis* Pb204.

Table 3.2: The Minimum bactericidal concentration (MBC) of eight different silver(I) phosphine complexes, the silver salt controls (silver nitrate and silver sulfadiazine) against *Enterobacter xiangfangensis* Pb204 and *Enterobacter xiangfangensis* LMG 27195^T.

MBC (mg/ml)		
	<i>E. xiangfangensis</i> LMG 27195 ^T	<i>E. xiangfangensis</i> Pb204
AgNO₃	0.03125	0.25
AgSD	0.03125	0.25
UJ1	0.25	>1
UJ2	>1	>1
UJ3	>1	>1
UJ4	>1	>1
UJ1A	>1	>1
UJ15	>1	>1
UJ34	>1	>1
UJ35	>1	>1

Antibacterial agents can be classified as either bactericidal or bacteriostatic. A bacteriostatic agent inhibits the growth of bacteria by keeping them in a stationary state followed by recovery, whereas a bactericidal agent eradicates the bacteria (Pankey and Sabath, 2004). The antibacterial properties (bacteriostatic vs bactericidal) of the silver(I) phosphine compounds and the positive antimicrobial controls were evaluated using the MBC/MIC ratio. A compound is considered bacteriostatic if the MBC/MIC ratio is greater than four. Contrary, when the MBC/MIC ratio is less than or equal to four the compound is considered to be bactericidal (Pipattanachat *et al.*, 2021). The MBC/MIC ratio for the treatments against the *E. xiangfangensis* LMG 27195^T and *E. xiangfangensis* Pb204 strains are displayed in Tables 3.3 and 3.4, respectively.

Table 3.3: The minimum bactericidal concentration/minimum inhibitory concentration ratio and the antibacterial effect of silver(I) phosphine compounds and the positive control silver salts against *Enterobacter xiangfangensis* LMG 27195^T.

Compound	MBC/MIC ratio	Antibacterial effect
AgNO ₃	2	Bactericidal
AgSD	2	Bactericidal
UJ1	2	Bactericidal
UJ2	>8	Bacteriostatic
UJ3	>8	Bacteriostatic
UJ4	>8	Bacteriostatic
UJ1A	>8	Bacteriostatic
UJ15	>8	Bacteriostatic
UJ34	>8	Bacteriostatic
UJ35	>8	Bacteriostatic

Table 3.4: The minimum bactericidal concentration/minimum inhibitory concentration ratio and antibacterial effects of silver(I) phosphine compounds and the positive control silver salts against the *Enterobacter xiangfangensis* Pb204.

Compound	MBC/MIC ratio	Antibacterial effect
AgNO ₃	8	Bacteriostatic
AgSD	4	Bactericidal
UJ1	>8	Bacteriostatic
UJ2	>8	Bacteriostatic
UJ3	>8	Bacteriostatic
UJ4	>8	Bacteriostatic
UJ1A	>8	Bacteriostatic
UJ15	>8	Bacteriostatic
UJ34	>8	Bacteriostatic
UJ35	>8	Bacteriostatic

Of all the silver(I) compounds tested, UJ1 was the only treatment that displayed bactericidal activity against *E. xiangfangensis* LMG 27195^T. The rest of the silver treatments were bacteriostatic with MBC/MIC ratios of above 4. However, for the *E. xiangfangensis* Pb204 strain, none of the silver(I) compounds displayed bactericidal activity. In contrast, both AgNO₃ and AgSD positive control silver salts showed a bactericidal effect against *E. xiangfangensis* LMG 27195^T with the same MBC/MIC ratio of 2. For the more resistant strain, *E. xiangfangensis* Pb204, only AgSD was considered bactericidal with an MBC/MIC ratio of 4, while that of AgNO₃ had a bacteriostatic effect with an MBC/MIC ratio of 8.

3.2 INVESTIGATING THE ANTI-BIOFILM ACTIVITY OF THE SILVER(I) PHOSPHINE COMPOUNDS.

3.2.1 CRYSTAL VIOLET ASSAY

The family of *Enterobacteriaceae* has been identified as the major cause of biofilm-associated infections. Biofilms formed by *E. xiangfangensis* strains on various abiotic surfaces, including medical devices, cause infections (Liu *et al.*, 2022; Ruhai and Kataria, 2021). A biofilm is considered a key virulence phenotype of ESKAPE pathogens; therefore, it is empirical to comprehend biofilm formation and find suitable antibiofilm molecules (Ruhai and Kataria, 2021). Here, a microtiter dish biofilm formation assay was done using crystal violet to assess the biofilm inhibitory action of the silver(I) phosphine compounds on the two *E. xiangfangensis* strains. The cells were co-incubated with the silver(I)phosphine compounds, silver salt controls at their MIC concentrations (reported in Table 3.1) and DMSO (25%)(v/v) vehicle control. Biofilm formation was monitored for 48 h. The percentage biofilm formation of *E. xiangfangensis* LMG 27195^T and *E. xiangfangensis* Pb204 when exposed to the various treatments is shown in Figure 3.1.

All the silver(I) phosphine compounds significantly ($p < 0.001$) inhibited biofilm formation of both strains when compared to the vehicle control. When comparing the two strains, the compounds demonstrated statistically significant better suppression of biofilm formation against *E. xiangfangensis* LMG 27195^T than *E. xiangfangensis* Pb204 ($p < 0.05$). In addition, the AgSD and AgNO₃ treatment inhibited the formation of biofilm to a greater extent in the *E. xiangfangensis* LMG 27195^T as compared to the *E. xiangfangensis* Pb204.

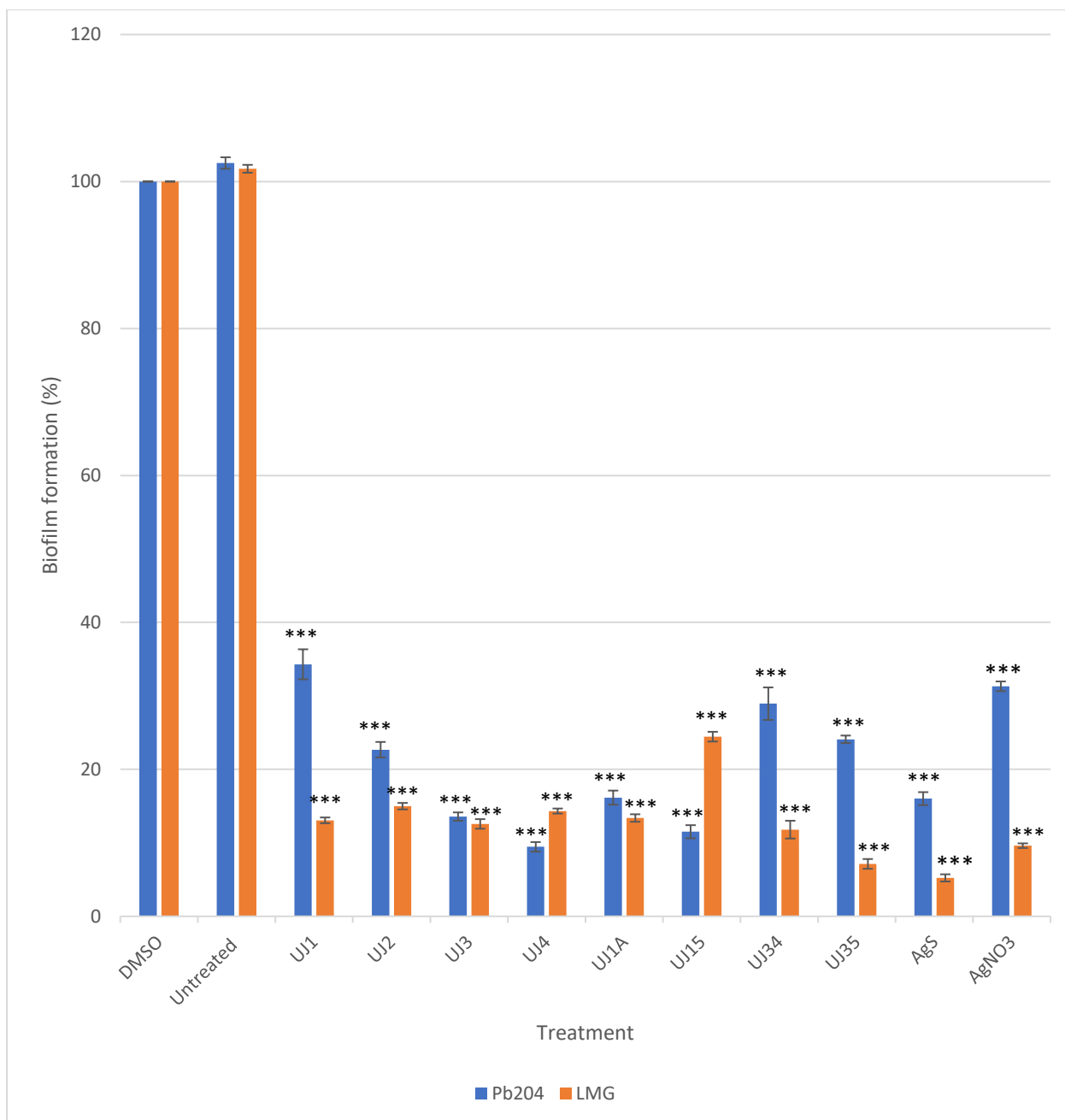


Figure 3.1: The inhibitory effects of various silver(I) phosphine complexes on *Enterobacter xiangfangensis* Pb204 and *Enterobacter xiangfangensis* LMG 27195^T biofilm formation when co-incubated for 48 h at their respective MIC concentrations. The DMSO (25%)(v/v) was used as a vehicle control and the percentage biofilm formation for each treatment were calculated with reference to the vehicle control. The silver nitrate and silver sulfadiazine salts (positive antimicrobial controls) were used. The error bars represent the standard error of mean (SEM; n = 9). The significant difference between the treated samples and the vehicle control were calculated using the student t-test (*** p<0.001)

Biological biofilm degradation is the process by which agents affect mature biofilms of pathogens (Song *et al.*, 2019). The bacterial cultures of *E. xiangfangensis* Pb204 and *E. xiangfangensis* LMG 27195^T were incubated in the 96-well microtiter plates for 48 h to allow the biofilms to form in the absence of any treatment. Following 48 h incubation, unattached cells were washed off the 96-well plate and the attached biofilms were treated with the silver (I) phosphine compounds at their MIC concentration (Table 3.1) for 24 h.

To determine the biofilm degradation properties of the complexes, the same crystal violet assay was used. In this assay, the percentage of biofilm degradation was calculated with respect to the DMSO (25%)(v/v) vehicle control (Figure 3.2). Based on the decreased absorbance, all the tested silver(I) phosphine compounds significantly ($p < 0.001$) degraded the biofilm mass formed by both strains when compared to the vehicle control. The percentage biofilm reduction effect of the silver(I)phosphine compounds was statistically significant when compared to the vehicle control for both strains ($p < 0.001$). Interestingly, the silver phosphine compounds had a better biofilm degradation effect than the AgNO₃ salt since the biofilm biomass percentage for the silver (I) phosphine treatments range between 13-25%, but for AgNO₃-treated biofilms the biomass was between 40-50% for both strains. However, when comparing the two strains, the maximum biofilm reduction was observed in *E. xiangfangensis* LMG 27195^T when treated with UJ1, UJ3, UJ4, UJ1A, UJ34, and UJ35. Moreover, the AgSD control induced biofilm degradation of *E. xiangfangensis* LMG 27195^T strain more effectively when compared to *E. xiangfangensis* Pb204.

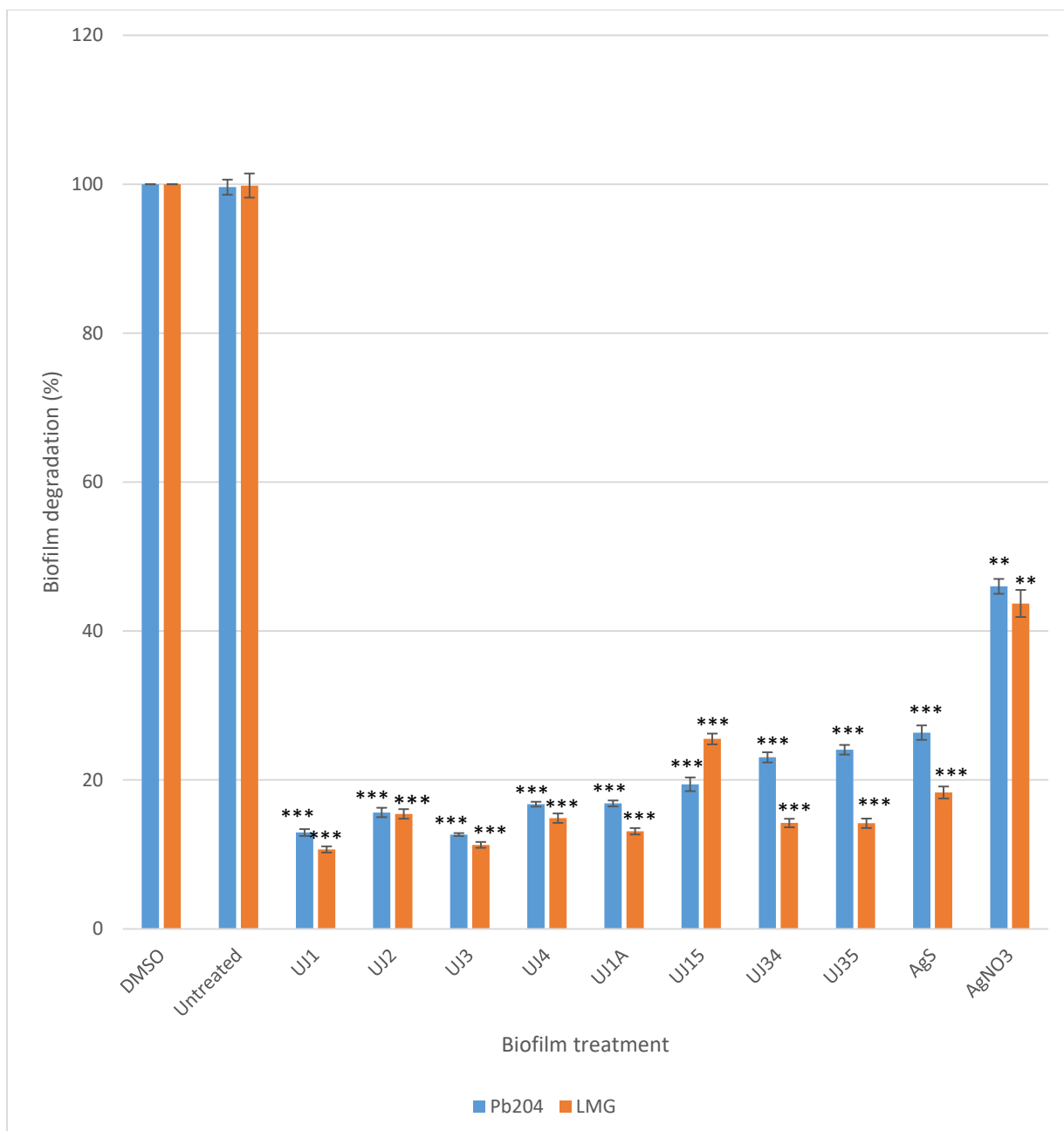


Figure 3.2: The effect of the silver(I) phosphine compounds on matured biofilms formed by *Enterobacter xiangfangensis* Pb204 and *Enterobacter xiangfangensis* LMG 27195^T. The biofilms were allowed to form in 48 h, thereafter, treated with the various silver(I) phosphine compounds, silver nitrate and silver sulfadiazine were used as positive control, and the untreated biofilms were regarded as negative control. The percentage biofilm degradation was calculated with respect to the vehicle control DMSO (25%)(v/v). The error bars represent the SEM (n = 9) and the significance difference is represented with an asterik (** p<0.01, *** p<0.001).

3.2.2 XTT ASSAY

To determine how the metabolic activity of the bacterial cells, as biofilms, is affected by the silver(I) phosphine compounds, a tetrazolium salt (XTT) assay was used. The cells were co-incubated with the different silver(I) phosphine treatments (similar to the biofilm inhibition assay) at their MIC concentrations to allow the biofilm to form in 48 h. With the XTT assay, the microbial cells convert the yellow XTT dye into a hesperidium-coloured formazan product. As such, the measured formazan absorption indicates metabolic (cellular) activity as it is directly proportional to the amount of metabolically active cells (Koban *et al.*, 2012). A reduced percentage metabolic activity was observed in bacterial biofilms formed on the samples treated with the silver(I) phosphine compounds as compared to the vehicle control, the percentage reduction in metabolic activity was statistically significant ($p < 0.01$) for both strains tested (Figure 3.3). However, the percentage reduction of metabolic activity was higher in *E. xiangfangensis* LMG 27195^T as compared to the *E. xiangfangensis* Pb204. Higher metabolic activity was observed in *E. xiangfangensis* Pb204 for all the treatments compared to the *E. xiangfangensis* LMG 27195^T.

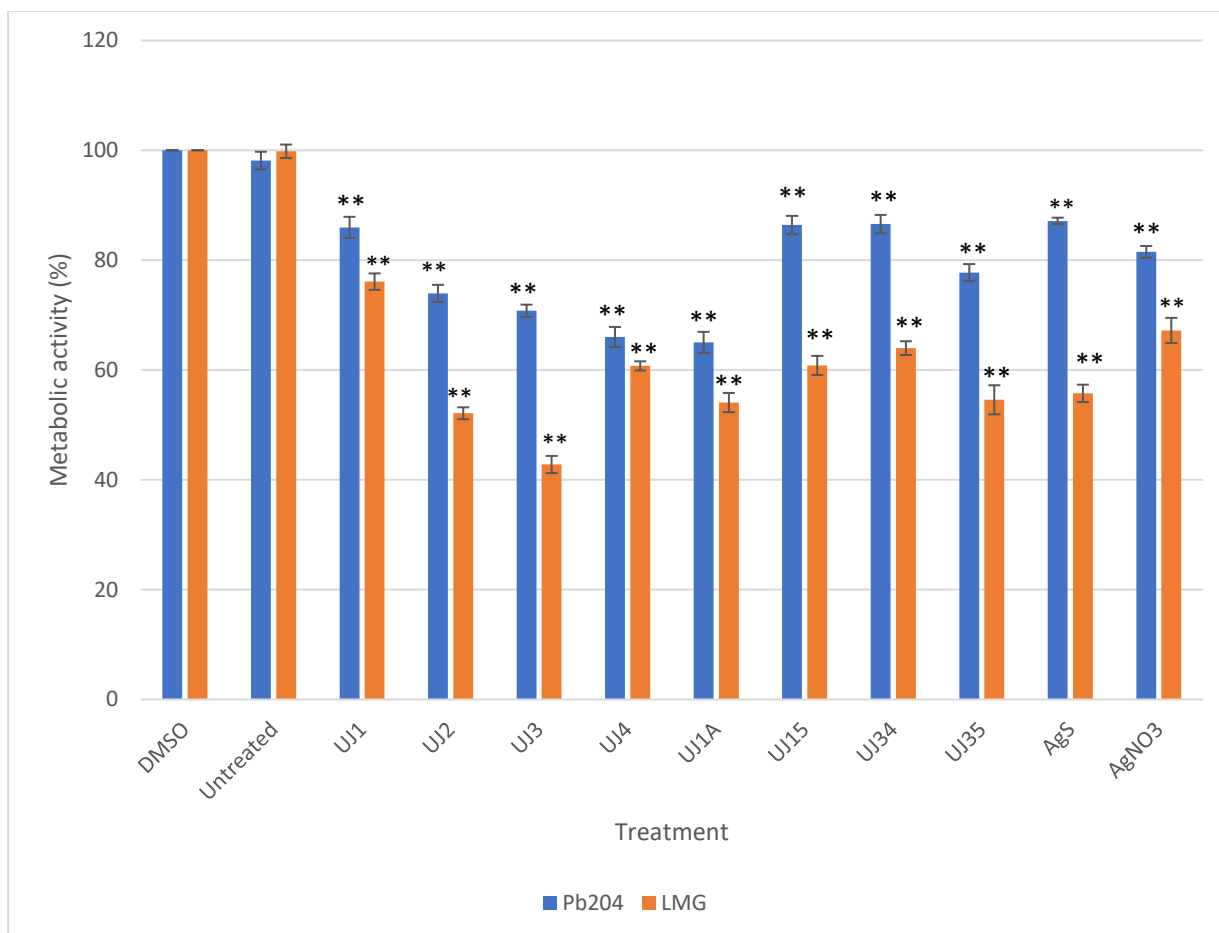


Figure 3.3: The metabolic activity of *Enterobacter xiangfangensis* Pb204 and *Enterobacter xiangfangensis* LMG 27195^T biofilms when co-incubated with different silver phosphine compounds. The untreated control, silver nitrate and silver sulfadiazine positive controls, and DMSO (25%) vehicle control was included. The cells were co-incubated with the treatments for 48 h to allow biofilm formation to take place. The percentage metabolic activity was calculated relative to DMSO (25%)(v/v) vehicle control. The error bars represent the standard error of mean (SEM, where n = 9). The significance difference between the DMSO(25%) vehicle control and treated samples was calculated using the student's t-test (** p<0.01)

As opposed to the planktonic bacteria, bacterial biofilm exhibit alterations in metabolic levels including decreased growth rate, altered gene expression and elevated EPS production (Misra *et al.*, 2022; Prakash *et al.*, 2003). To form biofilms, 200 μ L of *E. xiangfangensis* Pb204 and *E. xiangfangensis* LMG 27195^T bacteria culture was incubated in a 96-well plate and left to incubate for 48 h. This was then followed by treating the biofilms with various silver(I) phosphine compounds, including controls, at their MIC concentrations (Table 3.1). The XTT assay was done in order to evaluate the metabolic activity of *E. xiangfangensis* Pb204 and *E. xiangfangensis* LMG 27195^T

48 h formed biofilms when treated with the silver(I) phosphine compounds. The silver(I) phosphine compounds significantly ($p < 0.001$) reduced the metabolic activity of biofilms formed by both *E. xiangfangensis* strains (Figure 3.4). However, it should be noted that *E. xiangfangensis* LMG 27195^T treated biofilms showed a lower metabolic rate as compared to *E. xiangfangensis* Pb204.

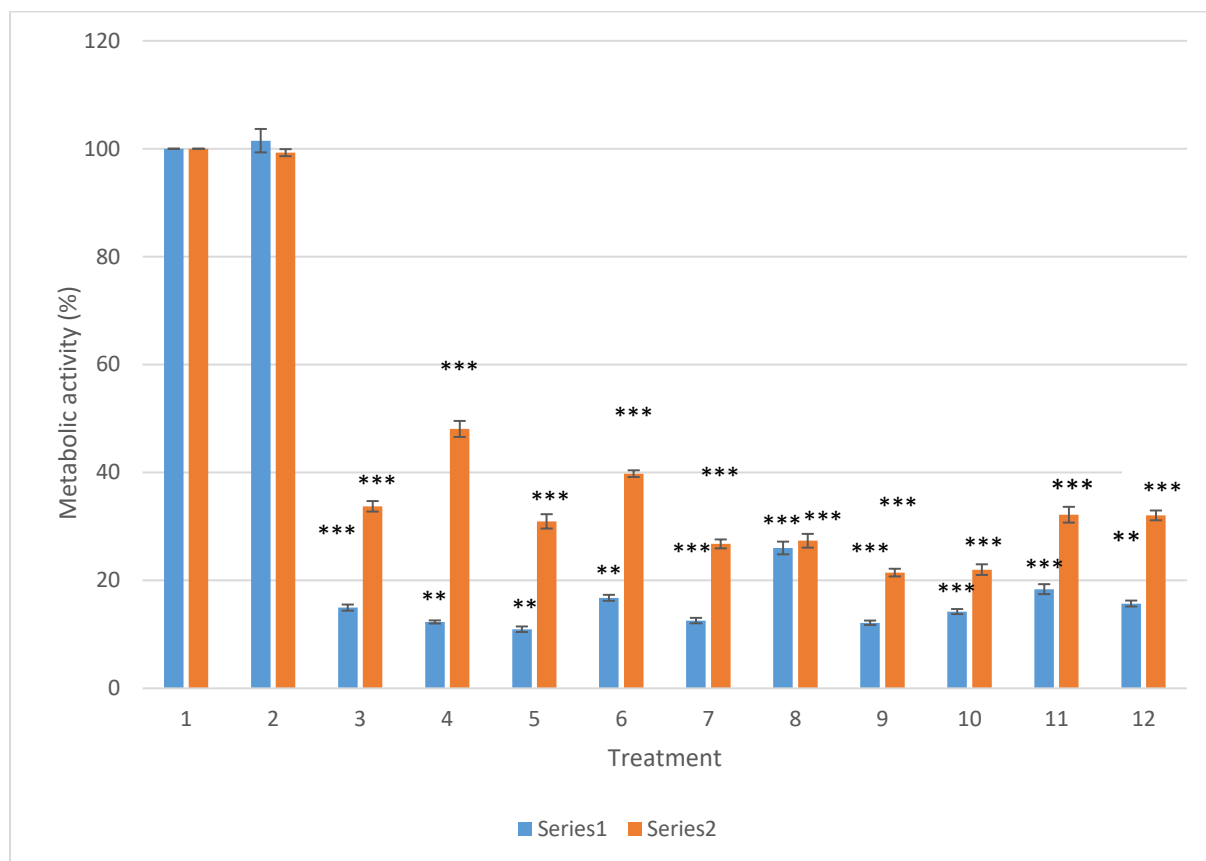


Figure 3.4: Metabolic activity of *Enterobacter xiangfangensis* Pb204 and *Enterobacter xiangfangensis* LMG 27195^T 48 h formed biofilms when treated with various silver(I) phosphine compounds at their MIC (Table 3.1). Silver nitrate and silver sulfadiazine were used as positive controls, untreated cells were included as negative control. Metabolic activity is conveyed as percentage relative to the vehicle control (25% DMSO)(v/v). The standard error of mean (SEM; $n = 9$) is presented as error bars. The significant difference was calculated using the student's t-test (** $p < 0.01$, *** $p < 0.001$)

3.3 GENE EXPRESSION STUDIES

The antibiotic susceptibility MIC (Table 3.1), antibiofilm (Figure 3.1 and 3.2) and metabolic activity (Figure 3.3 and 3.4) results show that the silver(I) phosphine compounds have antimicrobial effects against both *E. xiangfangensis* Pb204 and *E. xiangfangensis* LMG 27195^T. However, the results also reveal that the susceptibility of the two strains varies; *E. xiangfangensis* Pb204 was less susceptible to the silver(I) phosphine (UJ1 in particular) and positive silver salt control as compared to *E. xiangfangensis* LMG 27195^T as a higher concentration was needed for the compounds to exhibit a bactericidal effect (Table 3.2). The perceived extent of silver resistance of *E. xiangfangensis* Pb204 could be due to the expression of resistance genes (Randall *et al.*, 2015). According to genomic studies done previously, the whole genome of *E. xiangfangensis* Pb204 was found to be larger than that of *E. xiangfangensis* LMG 27195^T consisting of an additional ICE element containing genes coding for a silver resistance pathway (Ho *et al.*, 2018). To further understand the resistance mechanism of *E. xiangfangensis* Pb204, especially after being treated with silver(I) phosphine compounds, RT-qPCR was conducted to monitor the changes in the gene expression.

The cultured *E. xiangfangensis* Pb204 cells were treated with compound UJ1, AgSD or AgNO₃ using half the MIC of the compounds (Table 3.1), respectively. The treated cells were incubated for 16 h in order to have enough cells for extraction, since the compounds have antibacterial activity against this strain, longer incubation times would have completely inhibited all cell growth resulting in insufficient quantity of cells to harvest the RNA for RT-qPCR. The compound UJ1 and the AgNO₃ were selected because they demonstrated a bactericidal effect against *E. xiangfangensis* LMG 27195^T but was not bactericidal against *E. xiangfangensis* Pb204 (Table 3.3 and 3.4). The AgSD exhibited a bactericidal effect on both strains, however, it was chosen because the MIC and MBC required to exhibit a bactericidal effect on *E. xiangfangensis* Pb204 cells was higher as compared to *E. xiangfangensis* LMG 27195^T strain. Following 16 h treatment of the *E. xiangfangensis* Pb204 cells, RNA was extracted from the cells and quantified using a nanodrop as quantification gives information about the concentration and purity of the RNA (Table B1.1). Furthermore, the integrity of the RNA was assessed using an agarose gel in order to ensure that intact RNA was extracted and there was no gDNA contamination in the extracted RNA samples. The extracted RNA was pure and had no gDNA contamination (Figure B1.1).

The extracted RNA was then converted to cDNA to be used as a template for RT-qPCR. The level of gene expression of *silA*, *silR* and *silS* in *E. xiangfangensis* Pb204 treated with UJ1 and the positive silver controls (AgNO_3 and AgSD) was quantified using RT-qPCR, *gyrB* was used as a housekeeping gene for normalization. RT-qPCR allows the quantification of transcripts in real time, and due to its sensitivity and specificity levels of gene expression can be easily detected. The upregulation of the *silA*, *silR* and *silS* genes was noted when the *E. xiangfangensis* Pb204 cells were treated with the compound UJ1, AgNO_3 and AgSD (Figure 3.5). The observed changes in gene expression indicates that *E. xiangfangensis* Pb204 is less susceptible to the silver(I) phosphine compounds due to the upregulation of the genes involved in the silver resistance pathway.

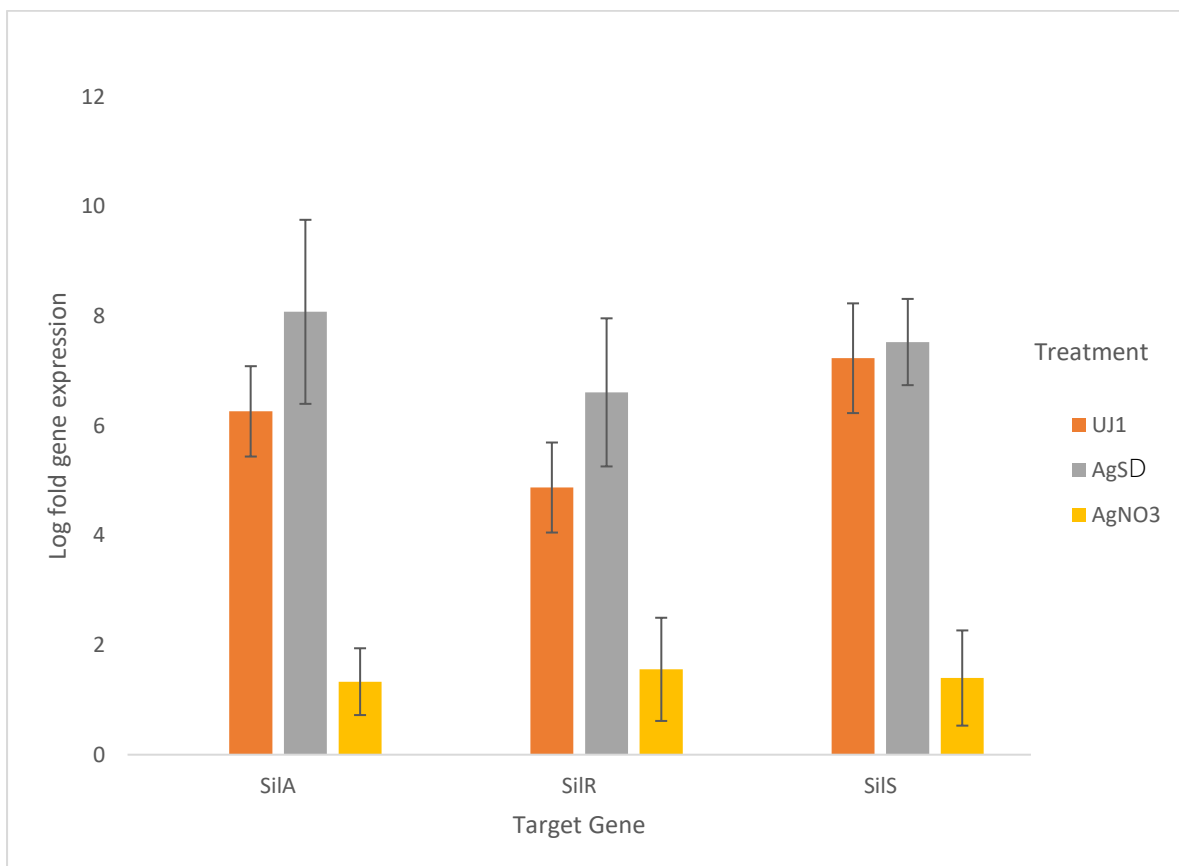


Figure 3.5: Log fold gene expression of three different genes (*silA*, *silR*, *silS*) encoded on the ICE element which codes for the activation of the silver resistance pathway in *Enterobacter xiangfangensis* Pb204. The cells were treated with UJ1 compound, silver sulfadiazine, and silver nitrate salts. The $\Delta\Delta\text{Ct}$ method was used to calculate the fold gene expression with respect to DMSO. The error bars signify the standard error of mean (SEM; n = 6)

3.4 COMPARATIVE GENOMICS

Using Orthofinder, the proteins encoded on the genomes of the two *E. xiangfangensis* strains were grouped into their orthologous groups. This approach aimed to investigate the potential differences in the proteins encoded in each bacterial strain. Through this analysis, the core proteins (protein orthologues shared by both strains) and protein unique to each strain were identified. The two strains share 3817 proteins which forms the core genome. Furthermore, the Pb204 strain encodes 458 unique proteins, whereas the LMG 27195^T strain has 290 unique proteins (Figure 3.6).

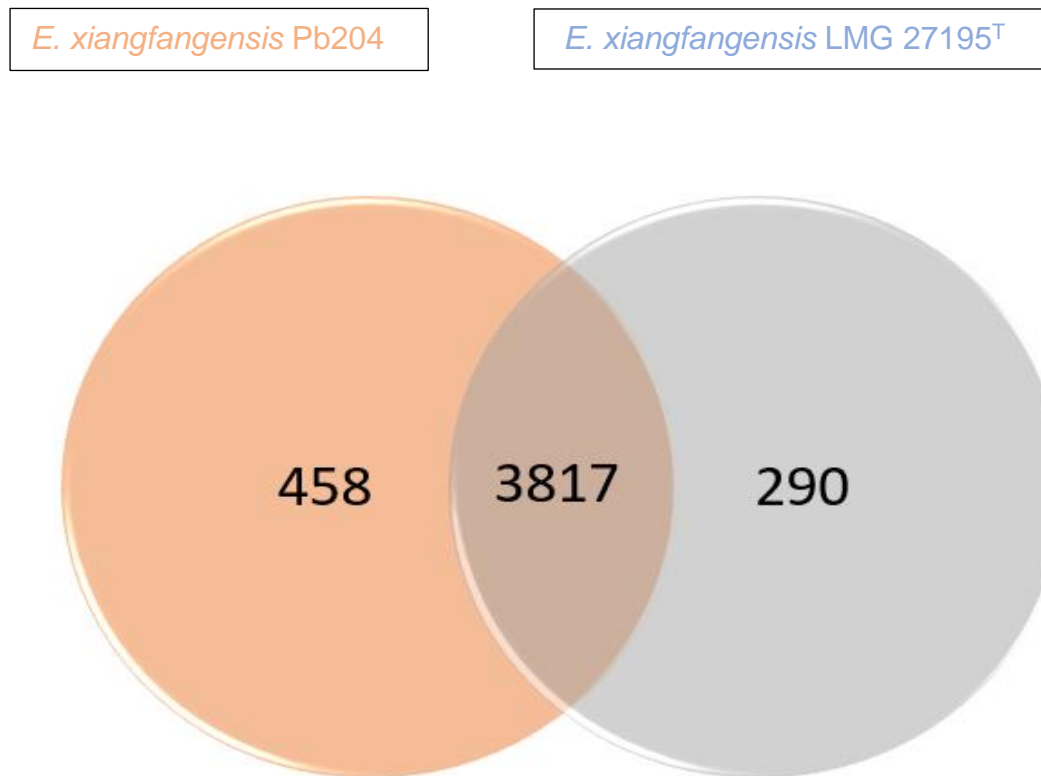


Figure 3.6: Venn diagram showing proteins that are shared (core proteins) between the two *Enterobacter xiangfangensis* strains and proteins that are unique to each strain. The orthologous proteins were analysed using OrthoFinder (Emms, 2019).

The orthologous proteins (core and unique) were functionally categorized in accordance with Conserved Orthologous Groups (COGs) using eggNOG mapper. According to eggNOG functional categorization, most of the proteins encoded on both genomes had an unknown function (Figure 3.7). Moreover, the proportion of functional classification of the core and unique proteins encoded by *E. xiangfangensis* Pb204 and *E. xiangfangensis* LMG 27195^T were at most indistinguishable indicating that the two genomes are highly conserved (Figure 3.7). The proteins which play a role in inorganic ion transport and metabolism enables the bacteria to utilize inorganic molecules such as metals (Drapeau and Macleod, 1965; van Vliet *et al.*, 2001), whilst proteins involved in defence mechanisms enable the bacteria to be more resistant to antimicrobials. The results obtained from the functional classification shows that *E. xiangfangensis* Pb204 had a slightly higher proportion of proteins involved in inorganic ion transport and metabolism. Conversely, *E. xiangfangensis* LMG 27195^T strain had a slightly higher proportion of proteins which plays a role in defence mechanisms (60 proteins) as compared to *E. xiangfangensis* Pb204 (40 proteins).

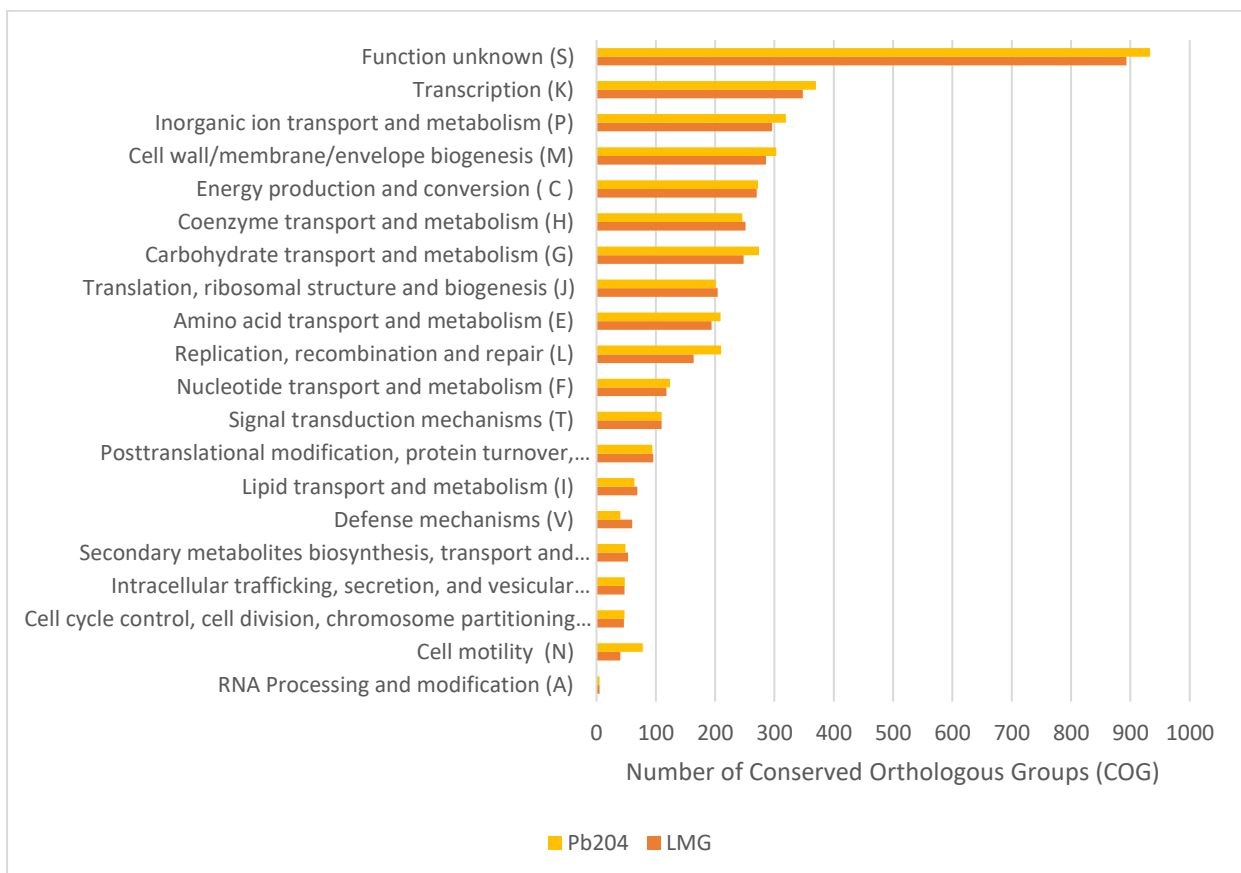


Figure 3.7: COG Classification of core and unique proteins encoded in the genomes of the compared *Enterobacter xiangfangensis* Pb204 and *Enterobacter xiangfangensis* LMG 27195^T. The eggNOG mapper server was used.

For more insight on the putative functional variation between the two strains, the genomes were further classified according to supra-functional COG. The supra-functional COG categories are information storage and processing, cellular processes and signalling, and metabolism (Huerta-Cepas *et al.*, 2017). The classified COG proteins (Figure 3.8) were further grouped into the aforementioned supra-functional categories; metabolism (C,E,F,G,H,I,P,Q), cellular processes and signalling (M,N,O,T,U,V), Information storage and processing (J,K,L) where the core proteins were regarded as proteins that are conserved between the two strains (Figure 3.8). The majority of core (conserved) proteins are involved in metabolism (52%), followed by information storage and processing (25%), and cellular processes and signalling (23%). The genomes of *E.xiangfangensis* Pb204 and *E.xiangfangensis* LMG 27195^T showed a similar pattern in terms of the distribution of COG composition (functional composition) (Figure 3.8).



Figure 3.8: Number of core and unique proteins encoded on the genomes of *Enterobacter xiangfangensis* Pb204 and *Enterobacter xiangfangensis* LMG 27195^T involved in metabolism, information storage and processing, as well as cellular processes and signalling functional categories.

However, when looking at the complete dataset of orthologous proteins encoded by *E. xiangfangensis* Pb204 there is an increase in the number of proteins involved in all the supra-functional COG categories as compared to *E. xiangfangensis* LMG 27195^T. A one-fold increase in proteins involved in metabolism, information storage and processing, as well as cellular processes and signalling was observed in *E. xiangfangensis* Pb204 protein coding sequence.

CHAPTER FOUR: DISCUSSION

The rapid emergence of MDR in bacteria, combined with the scarcity of effective new antibiotics in the field of drug development, necessitates strategies to address this critical issue. Researchers have been exploring inorganic medicinal chemistry as an avenue to investigate the potential of inorganic molecules as antimicrobial agents (Blanco *et al.*, 2016; Evans and Kavanagh, 2021; Olivier *et al.*, 2018; O'Shaughnessy *et al.*, 2020). Silver, a well-known antimicrobial, is widely used in the medical industry and is currently being applied to hospital surfaces to control and eradicate nosocomial infections (Barras, Aussel and Ezraty, 2018). The use of silver medicinally dates to the 17th century, where silver nitrate has been utilized to treat *Chlamydia trachomatis* which causes neonatal conjunctivitis (Frei *et al.*, 2023). Recently, silver sulfadiazine is the most widely used silver compound medicinally, it is used to treat skin burns and prevent infections (Oaks and Cindass, 2023). Further, numerous studies have reported the potency of various silver nanoparticles (AgNPs) and silver(I) compounds against Gram-negative and Gram-positive bacteria. However, the mechanism of action of these silver-based compounds is not fully understood (Ortego *et al.*, 2015b). Additionally, the advent of silver resistance has been identified as a major concern when it comes to long-term exposure of bacteria to silver compounds. In *Enterobacter* spp., silver resistance was found to be due to the overexpression of the *sil* operon (Randall *et al.*, 2015)

4.1 ANTIBACTERIAL ACTIVITY OF SILVER(I) PHOSPHINE COMPOUNDS

In this study, the results shows that the silver(I) phosphine compounds have antibacterial properties against *E. xiangfangensis* Pb204 and *E. xiangfangensis* LMG 27195^T. All the tested silver(I) phosphine compounds were bacteriostatic effect against *E. xiangfangensis* Pb204 meaning that they inhibit cell growth but do not completely kill the cells. According to the literature, the bacteriostatic effect is often due to the inhibition of bacterial protein synthesis pathways (Pankey and Sabath, 2004). Ag ions have a high affinity to sulfhydryl residues and the s-silver bond formed leads to protein inhibition in bacterial cells (Arakawa *et al.*, 2001). Therefore, the silver(I) phosphine compounds could putatively inhibit the protein synthesis pathway in the *E. xiangfangensis* species henceforth causing a bacteriostatic effect. In a study by Ortego and coworkers (2015), Ag(I) aminophosphane compounds were reported to have antibacterial activity against selected Gram-positive *S. aureus* ATCC 11632 *L. monocytogenes* EGD-e and Gram-negative *E. coli* ATCC 10536 and *S. typhimurium*

SV5015 bacteria. However, the compounds were more selective towards the Gram-positive pathogens and thus it was proposed that compounds could inhibit peptidoglycan synthesis in the cell wall of Gram-positive bacteria as the mechanism of action (Ortego *et al.*, 2015b).

Silver saccharinate complexes have also been found to have a bacteriostatic and bactericidal effect against *S. aureus*, *E. coli* and *S. typhimurium*. The study suggests that the ability of the Ag(I) complexes to inhibit bacterial growth is attributed to its DNA binding affinity since Ag ions have a high affinity to bind to nucleic acids resulting in DNA modification, as a result, bacterial replication is inhibited since the bacteria is subjected to mutations (Arakawa *et al.*, 2001; Evans and Kavanagh, 2021; Medici *et al.*, 2016).

Silver complexes' ability to kill bacteria cells is directly related to their water solubility and stability, lipophilicity, redox capacity, and rate of silver ion release (Medici *et al.*, 2016). The silver(I) phosphine compounds are lipophilic, and the compound UJ1 was the only compound that exhibited a bactericidal effect against *E. xiangfangensis* LMG 27195^T, strain (Table 3.3). This effect was comparable to the antimicrobial reference agents (AgNO₃ and AgSD) used in this study.

The rapid rate of ligand interchange of the metal ion in the biological organization is what gives silver(I) complexes their antibacterial capabilities. This relates to the type of donor atoms that were coordinated to the silver salt (Altaf *et al.*, 2013). Therefore, the rate of ion exchange when *E. xiangfangensis* LMG 27195^T cells are exposed to UJ1 could be higher as compared to the other compounds tested. The bactericidal effect of Ag is due to its propensity to interact with cysteine residues and thus induce protein impairment (Ortego *et al.*, 2015). Cysteine residues are often metalloproteins implicated in bacterial replication, metabolism, respiration and membrane structure (Arakawa *et al.*, 2001; Evans and Kavanagh, 2021; Ortego *et al.*, 2015). It has also been reported that the bactericidal effect of Ag is attributed to its ability to produce reactive oxygen species (ROS), however, the literature is still unclear on this (Evans and Kavanagh, 2021). Moreover, a compound will have a bactericidal effect if it is able to electrostatically interact with the bacteria's cell wall. Since Gram-positive bacteria have a thin outer membrane, the compound can easily interact with the cell wall as compared to Gram-negative bacteria, hence most reported metal compounds

selectively have profound antibacterial activity against Gram-positive bacteria (Altaf *et al.*, 2013; Ortego *et al.*, 2015b). However, little is reported about the antibacterial effects of metal or silver-based compounds against *E. xiangfangensis* strains.

4.2 ANTIBIOFILM ACTIVITY

In most clinical settings, about 65-80% of nosocomial infections are attributed to biofilm forming ESKAPE pathogens (Mezzatesta *et al.*, 2012). Biofilm formation is regarded as a key phenotype which contributes to AMR and the virulent nature of these pathogens (Chandki *et al.*, 2011). As such, bacterial biofilms pose a considerable threat to public health as they enable bacteria to resist current antibiotics. The use of biofilm inhibitors helps eradicate infections caused by biofilm-forming pathogens. Conventional antibiotics often have a low penetration capacity and weakened activity in the acidic microenvironments of a biofilm (Wu *et al.*, 2019). According to research, silver and copper nanoparticles can stop the growth of biofilms, making them useful as coverings for implants to reduce the risk of infections (Wu *et al.*, 2019). In this study, the antibiofilm activity of silver(I) phosphine compounds were investigated. The silver (I) phosphine compounds significantly inhibited biofilm formation of both *E. xiangfangensis* Pb204 and *E. xiangfangensis* LMG 27195^T. The inhibitory activity of all the tested silver (I) phosphine compounds outperformed the reference antibacterial silver salts AgNO₃ (Figure 3.1). Our results were consistent with the results of the study done by O'Shaughnessy (2020) where the antibiofilm activity of Ag (I) tdda-phen chelate ((tddaH₂ = 3,6,9-trioxaundecanedioic acid; phen = 1,10-phenanthroline) compounds was investigated. The study found that the Ag (I) tdda-phen complexes inhibit the biofilm formation of Gram-negative *P. aeruginosa* clinical isolates (O'Shaughnessy *et al.*, 2020). Furthermore, a study by Siddique and coworkers (2020) reported that biofilm formation was inhibited by 64% in *K. pneumoniae* MF953600 and 86% for *K. pneumoniae* MF953599 when pre-treated with 100 µg/ml of AgNPs. In addition, the study revealed that *K. pneumoniae* was unable to form biofilms when treated with 75 µL/ml of AgNPs (Siddique *et al.*, 2020). It was further concluded that this was due to the disruption of the EPS matrix (Siddique *et al.*, 2020).

When a biofilm is formed, the EPS inhibits or delays the entry of antibiotics into the bacterial clusters embedded in the biofilm (Miškovská *et al.*, 2022). The silver(I) phosphine compounds potentially disrupt established biofilms (post-treated) (Figure

3.2). The responsive assembly of Ag nanoclusters (rAgNAs) have been reported to significantly reduce the biomass of matured biofilms formed by MRSA. The authors concluded that the antibiofilm activity of rAgNAs is due to the use of structural disintegration to enhance the leaching of silver ions and an acidic microenvironment to increase the bactericidal impact locally (Wu *et al.*, 2019).

The silver(I) phosphine compounds putatively inhibit biofilm formation and disrupt mature biofilm in *E. xiangfangensis* Pb204 and *E. xiangfangensis* LMG 27195^T (Figure 3.1 and 3.2). The antibiofilm activity of the silver(I) phosphine compounds outperformed the silver salt AgNO₃, however, they were comparable to AgSD control (Figure 3.2). Planktonic cells are less resistant to antimicrobial agents as compared to cells in biofilms (Mistra, 2022). As a result, it is more difficult to disrupt or inhibit cells in established biofilms as compared to inhibiting cell attachment (biofilm formation) (Sharma *et al.*, 2019).

According to the literature, the metabolic activity of cells in biofilms is low due to limited oxygen and nutrient supply. The reduced metabolic activity accounts for the resistance of biofilms to antimicrobial agents (Chandki *et al.*, 2011; Prakash *et al.*, 2003). In our study, the silver(I) phosphine compounds studied had a significant impact on the metabolic activity of the cells forming the biofilms at ½ MIC of the respective compounds (Figure 3.3). The XTT results shows that the compounds reduced the metabolic activity of cells during biofilm formation and in pre-formed biofilms. In a study by Pourhajibagher and coworkers (2016), the XTT reduction was used to analyse the metabolic activity of *E. faecalis* biofilm when treated with ½ MIC of photodynamic therapy and a reduced metabolic activity was reported. Essential oils have also been reported to have an antibiofilm activity, a reduced metabolic activity was reported on *E. coli* and *S. aureus* biofilms treated with 1.6 µL/ml and 0.8 µL/ml, respectively (Bazargani and Rohloff, 2016). This reduction suggests a potential decrease in the number of viable bacterial cells. Interestingly, the metabolic activity of biofilm-forming cells was particularly more pronounced in the *E. xiangfangensis* LMG 27195^T than the *E. xiangfangensis* Pb204 (Figure 3.3), this suggests that the compounds are more effective on *E. xiangfangensis* LMG 27195^T. Our findings were consistent with the other studies where the crystal violet assays showed biofilm inhibition and degradation, and the XTT assay confirmed reduction in metabolic activity (Bazargani and Rohloff, 2016; Song *et al.*, 2019). To our knowledge this is the first study that

reported the antibiofilm activity of silver(I) phosphine compounds against biofilm formed by *E. xiangfangensis* Pb204 and *E. xiangfangensis* LMG 27195^T. Moreover, there is a huge knowledge gap on other molecules that can have an antibiofilm activity against the specific strain studied here.

4.3 SILVER RESISTANCE PATHWAY

The response of *E. xiangfangensis* Pb204 shows that it is resistant to silver as opposed to *E. xiangfangensis* LMG 27195^T. Resistance to silver is often a consequence of horizontal gene transfer or mutation and it was first characterized in *Salmonella typhimurium* which caused an outbreak in 1975 (Randall *et al.*, 2015). Silver resistance genes have been assigned to the *sil* operon which consists of two regulatory genes (*silS* and *silR*) and seven structural genes (*silA*, *silB*, *silC*, *silE*, *silF*, *silP* and *ORF105*) (Ho *et al.*, 2018; Randall *et al.*, 2015). The *sil* operon's proteins are thought to mediate Ag resistance by preventing Ag from building up inside the cell by a combination of silver sequestration in the periplasm and active efflux (Gupta *et al.*, 2001). Lok and coworkers, delineated Ag resistance in five *E.coli* mutants which showed a more than 60-fold reduction in Ag susceptibility compared with the wild-type strain. The study concluded that the reduced susceptibility to Ag is due to the loss of expression of outer membrane porins. As a result, the ingress of Ag into the cell wall is restricted (Lok *et al.*, 2008).

The silver(I) phosphine compounds tested displayed antibacterial and antibiofilm activity against *E. xiangfangensis* Pb204 and *E. xiangfangensis* LMG 27195^T. However, *E. xiangfangensis* LMG 27195^T was found to be more susceptible to the compounds as compared to *E. xiangfangensis* Pb204. The compound UJ1 had a bactericidal effect towards, *E. xiangfangensis* LMG 27195^T, contrary, *E. xiangfangensis* Pb204 was found to be resistant as this compound did not have a bactericidal effect against this strain. Furthermore, the MIC of AgNO₃ treated *E. xiangfangensis* Pb204 was higher as compared to *E. xiangfangensis* LMG 27195^T treated with AgNO₃. In a study by Randall and coworkers (2015), the MIC of AgNO₃ for *Enterobacter cloacae* was found to be 4 mg/mL which was higher when compared to the bacterial isolates which lack the *sil* operon (Randall *et al.*, 2015). This further justifies that the presence of a *sil* operon reduces the susceptibility of bacteria to silver molecules. Li and coworkers (2022) also described the selection of *E. coli* mutants which showed a reduction in Ag susceptibility compared to the type of strain. Clinical

isolates of *Enterobacter spp.* and *Klebsiella spp.* expressed silver resistance when treated with 128 mg/L of AgNO₃ (Selem *et al.*, 2022).

The genome of *E. xiangfangensis* Pb204 comprises of a multi-heavy-metal resistance pathway (sil, cop, znu) which is encoded on the ICE element (Ho *et al.*, 2018). Following the gene expression studies where *silR*, *silS* and *silA* genes were quantified, the expression of these genes was upregulated when *E. xiangfangensis* Pb204 cells were treated with 0.0625 mg/mL compound UJ1, 0.0156 mg/mL AgNO₃ and 0.03125 mg/ml AgSD (Figure 3.5). As expected, the expression of these genes were low in the untreated samples, and studies have shown that the silver pathway is repressed in the absence of a stimulus (Gupta *et al.*, 2001). When these genes are upregulated, it means that the Ag resistance pathway is indeed activated. The hypothesized mechanism of the silver pathway involves the binding of silver to the silE protein, which then activates the sensory histidine kinase silS. Subsequently, the silR response regulator protein becomes switched on and ultimately activates the silA efflux pump (Gupta *et al.*, 2001; Ho *et al.*, 2018a; Lok *et al.*, 2008; Randall *et al.*, 2015; Wang *et al.*, 2022). It's worth noting that the activation of the silA efflux alone is not adequate to accomplish an evident resistance phenotype. This is because the rate at which the efflux pumps out Ag is normally slower than the rate at which Ag is administered into the periplasm (Gupta *et al.*, 2001; Randall *et al.*, 2015). Therefore, for cells to possess a fully evident Ag resistance phenotype, the activation of Ag efflux pumps needs to be coupled with mechanisms which combat the aggregation of Ag ions in the periplasm (Wang *et al.*, 2022). While it is evident that the Ag resistance pathway is upregulated in *E. xiangfangensis* Pb204, our findings suggest that the Ag resistance phenotype in this strain cannot be solely attributed to this pathway. It appears that there are other additional genetic factors at play that enhance the efficacy of silver efflux in conferring resistance.

4.4 COMPARATIVE GENOMICS

Comparative genomics was executed to compare the genome of *E. xiangfangensis* Pb204 to *E. xiangfangensis* LMG 27195^T in order to pinpoint the similarities and differences between these strains. It was observed that the number of proteins, shared between the two strains, was higher compared to the number of unique proteins found in each individual strain (Figure 3.6). This implies that there is high genetic conservation between *E. xiangfangensis* Pb204 and *E. xiangfangensis* LMG 27195^T

strain. Moreover, the comparative genomics analysis revealed that *E. xiangfangensis* Pb204 harbours more unique proteins as compared to *E. xiangfangensis* LMG 27195^T. The variable genomic features between them could contribute to the perceived differences in susceptibility to silver as *E. xiangfangensis* Pb204 shifted to gain more genetic material coding for metabolism. The dominance of metabolism proteins is ascribed mainly to inorganic ion transport and metabolism (P), followed by carbohydrate transport and metabolism (G) and energy production and conversion (C) (Figure 3.7). Excess and lack of ions may cause cellular stress which often inhibits cell growth or induces cell death (van Vliet *et al.*, 2001). As such, bacteria moderate the uptake, storage, usage and efflux of ions in order to maintain its ion homeostasis (van Vliet *et al.*, 2001). *E. xiangfangensis* Pb204 has diversified in terms of the inorganic ion and carbohydrates transport they utilize. Transport channels are essential for Gram-negative bacteria since their outer membrane prevents molecules from entering the cells passively, therefore, these channels facilitates the translocation of ions into the cell (Frei *et al.*, 2023). Moreover, it has been shown that the ICE_{XiPb204} element encodes for metabolic adaptation and antibiotic resistance (De Maayer *et al.*, 2017; Ho *et al.*, 2018a) .

CHAPTER FIVE: CONCLUSION

5.1 CONCLUSION

The silver(I) phosphine compounds studied herein exhibit distinct profiles of antibacterial activity against *E. xiangfangensis* Pb204 and *E. xiangfangensis* LMG 27195^T. Seven of the tested compound's activity was considered bacteriostatic against both bacterial strains. UJ1 was the only compound with bactericidal activity against *E. xiangfangensis* LMG 27195^T making it a promising antimicrobial agent. However, *E. xiangfangensis* Pb204 was found to be more resistant to silver as the MIC values indicated that a higher concentration of the silver salts (AgNO₃ and AgSD) was required for it to be susceptible. In addition, UJ1 was not able to induce a bactericidal effect against this strain. Furthermore, the results from the crystal violet and XTT assays revealed that the silver(I) phosphine compounds inhibit biofilm formation, degrade pre-formed biofilms and reduce metabolic activity in biofilm cells. This shows that the silver(I) phosphine compounds have clinical significance as they inhibit biofilm formation and degrade pre-formed biofilms. However, *E. xiangfangensis* Pb20 biofilms are less susceptible to the silver treatments compared to *E. xiangfangensis* LMG 27195^T. Gene expression studies showed that the silver resistance in *E. xiangfangensis* Pb204 is due to the upregulation of the *sil* operon which activates the silver resistance pathway. Moreover, *E. xiangfangensis* Pb204 has evolved to have more proteins coding for ion transport and carbohydrates to survive in harsh conditions that have high concentrations of heavy metals.

5.2 FUTURE STUDIES

Considering the bactericidal effect of UJ1 against the *E. xiangfangensis* LMG 27195^T, it is strongly recommended that the mechanism of action should be elucidated. Building on previous studies that indicate the binding of silver to nucleic acids, resulting in DNA modification (Randall *et al.*, 2015) thermodynamic experiments should be completed to ascertain whether the silver(I) phosphine, specifically UJ1, form any bonds with nucleic acids. Though these experiments, crucial insights can be obtained regarding the interaction between UJ1 and nucleic acids, shedding light on how their potential mechanism of action and DNA-modifying properties. Moreover, fluorescence microscopy with UJ1-treated cells would help confirm if there are any changes in the DNA found in the centre of the cell. Transmission electronic microscopy (TEM) may be conducted to assess if the UJ1- treated cells have any structural or morphological changes in the cell membrane.

Furthermore, in the study, RT-qPCR was done to evaluate the expression of genes in the *sil* operon. However, *E. xiangfangensis* LMG 27195^T lacks the *sil* operon, future studies using RNA-seq of this strain, treated silver(I) phosphine compounds, should be conducted. This will enable one to identify all the genes which are differentially expressed in the transcriptome of the bacterial species. Such analysis would provide valuable insights into the specific genes influenced by silver(I) phosphine compounds, aiding in the understanding of the molecular basis of susceptibility in *E. xiangfangensis* LMG 27195^T and further elucidating the resistance mechanisms of *the E. xiangfangensis* Pb204. Lastly, the compounds should be screened against more clinical isolates on *Enterobacter xiangfangensis* as well as other ESKAPE pathogens in order to assess their efficacy against a broader range of organisms.

REFERENCES

- Alexander, J.W., 2009. History of the Medical Use of Silver. *Surg. Infect.* 10, 289–292. <https://doi.org/10.1089/sur.2008.9941>
- Altaf, M., Stoeckli-Evans, H., Cuin, A., Sato, D.N., Pavan, F.R., Leite, C.Q.F., Ahmad, S., Bouakka, M., Mimouni, M., Khardli, F.Z., Hadda, T.B., 2013. Synthesis, crystal structures, antimicrobial, antifungal and antituberculosis activities of mixed ligand silver(I) complexes. *Polyhedron* 62, 138–147. <https://doi.org/10.1016/j.poly.2013.06.021>
- Annavajhala, M.K., Gomez-Simmonds, A., Uhlemann, A.-C., 2019. Multidrug-Resistant *Enterobacter cloacae* Complex Emerging as a Global, Diversifying Threat. *Front. Microbiol.* 10.
- Ansel, H.C., Norred, W.P., Roth, I.L., 1969. Antimicrobial activity of dimethyl sulfoxide against *Escherichia coli*, *Pseudomonas aeruginosa*, and *Bacillus megaterium*. *J. Pharm. Sci.* 58, 836–839. <https://doi.org/10.1002/jps.2600580708>
- Arakawa, H., Neault, J.F., Tajmir-Riahi, H.A., 2001. Silver(I) complexes with DNA and RNA studied by Fourier transform infrared spectroscopy and capillary electrophoresis. *Biophys. J.* 81, 1580–1587.
- Ares, M., 2012. Bacterial RNA isolation. *Cold Spring Harb. Protoc.* 2012, 1024–1027. <https://doi.org/10.1101/pdb.prot071068>
- Arya, M., Shergill, I.S., Williamson, M., Gommersall, L., Arya, N., Patel, H.R.H., 2005. Basic principles of real-time quantitative PCR. *Expert Rev. Mol. Diagn.* 5, 209–219. <https://doi.org/10.1586/14737159.5.2.209>
- Aziz, R.K., Bartels, D., Best, A.A., DeJongh, M., Disz, T., Edwards, R.A., Formsma, K., Gerdes, S., Glass, E.M., Kubal, M., Meyer, F., Olsen, G.J., Olson, R., Osterman, A.L., Overbeek, R.A., McNeil, L.K., Paarmann, D., Paczian, T., Parrello, B., Pusch, G.D., Reich, C., Stevens, R., Vassieva, O., Vonstein, V., Wilke, A., Zagnitko, O., 2008. The RAST Server: rapid annotations using subsystems technology. *BMC Genomics* 9, 75. <https://doi.org/10.1186/1471-2164-9-75>
- Balfourier, A., Kolosnjaj-Tabi, J., Luciani, N., Carn, F., Gazeau, F., 2020. Gold-based therapy: From past to present. *Proc. Natl. Acad. Sci.* 117, 22639–22648. <https://doi.org/10.1073/pnas.2007285117>

- Balouiri, M., Sadiki, M., Ibsouda, S.K., 2016. Methods for in vitro evaluating antimicrobial activity: A review. *J. Pharm. Anal.* 6, 71–79. <https://doi.org/10.1016/j.jpha.2015.11.005>
- Barillo, D.J., Marx, D.E., 2014. Silver in medicine: A brief history BC 335 to present. *Burns, Silver in Wound Care: A Review of the State of the Art* 40, S3–S8. <https://doi.org/10.1016/j.burns.2014.09.009>
- Bazargani, M.M., Rohloff, J., 2016. Antibiofilm activity of essential oils and plant extracts against *Staphylococcus aureus* and *Escherichia coli* biofilms. *Food Control* 61, 156–164. <https://doi.org/10.1016/j.foodcont.2015.09.036>
- Benedek, T., 2004. The History of Gold Therapy for Tuberculosis. *J. Hist. Med. Allied Sci.* 59, 50–89. <https://doi.org/10.1093/jhmas/59.1.50>
- Blanco, P., Hernando-Amado, S., Reales-Calderon, J.A., Corona, F., Lira, F., Alcalde-Rico, M., Bernardini, A., Sanchez, M.B., Martinez, J.L., 2016. Bacterial Multidrug Efflux Pumps: Much More Than Antibiotic Resistance Determinants. *Microorganisms* 4, 14. <https://doi.org/10.3390/microorganisms4010014>
- Bonev, B., Hooper, J., Parisot, J., 2008. Principles of assessing bacterial susceptibility to antibiotics using the agar diffusion method. *J. Antimicrob. Chemother.* 61, 1295–1301. <https://doi.org/10.1093/jac/dkn090>
- Brettin, T., Davis, J.J., Disz, T., Edwards, R.A., Gerdes, S., Olsen, G.J., Olson, R., Overbeek, R., Parrello, B., Pusch, G.D., Shukla, M., Thomason, J.A., Stevens, R., Vonstein, V., Wattam, A.R., Xia, F., 2015. RASTtk: a modular and extensible implementation of the RAST algorithm for building custom annotation pipelines and annotating batches of genomes. *Sci. Rep.* 5, 8365. <https://doi.org/10.1038/srep08365>
- Cantalapiedra, C.P., Hernández-Plaza, A., Letunic, I., Bork, P., Huerta-Cepas, J., 2021. eggNOG-mapper v2: Functional Annotation, Orthology Assignments, and Domain Prediction at the Metagenomic Scale. *Mol. Biol. Evol.* 38, 5825–5829. <https://doi.org/10.1093/molbev/msab293>
- Chandki, R., Banthia, P., Banthia, R., 2011. Biofilms: A microbial home. *J. Indian Soc. Periodontol.* 15, 111–114. <https://doi.org/10.4103/0972-124X.84377>

De Maayer, P., Aliyu, H., Vikram, S., Blom, J., Duffy, B., Cowan, D.A., Smits, T.H.M., Venter, S.N., Coutinho, T.A., 2017. Phylogenomic, Pan-genomic, Pathogenomic and Evolutionary Genomic Insights into the Agronomically Relevant *Enterobacteria Pantoea ananatis* and *Pantoea stewartii*. *Front. Microbiol.* 8.

De Maayer, P., Chan, W.-Y., Martin, D.A.J., Blom, J., Venter, S.N., Duffy, B., Cowan, D.A., Smits, T.H.M., Coutinho, T.A., 2015. Integrative conjugative elements of the ICEPan family play a potential role in *Pantoea ananatis* ecological diversification and antibiosis. *Front. Microbiol.* 6, 576. <https://doi.org/10.3389/fmicb.2015.00576>

Dell, A.J., Navsaria, P.H., Gray, S., Kloppers, J.C., 2020. Nosocomial infections: A further assault on patients in a high-volume urban trauma centre in South Africa. *S. Afr. Med. J.* 110, 123–125. <https://doi.org/10.7196/SAMJ.2020.v110i2.14243>

Denman, S.E., McSweeney, C.S., 2005. Quantitative (real-time) PCR, in: Makkar, H.P.S., McSweeney, C.S. (Eds.), *Methods in Gut Microbial Ecology for Ruminants*. Springer Netherlands, Dordrecht, pp. 105–115. https://doi.org/10.1007/1-4020-3791-0_8

Dilruba, S., Kalayda, G.V., 2016. Platinum-based drugs: past, present and future. *Cancer Chemother. Pharmacol.* 77, 1103–1124. <https://doi.org/10.1007/s00280-016-2976-z>

Drapeau, G.R., Macleod, R.A., 1965. A Role for Inorganic Ions in the Maintenance of Intracellular Solute Concentrations in a Marine Pseudomonad. *Nature* 206, 531–531. <https://doi.org/10.1038/206531a0>

Eloff, J., 1999. A Sensitive and Quick Microplate Method to Determine the Minimal Inhibitory Concentration of Plant Extracts for Bacteria. *Planta Med.* 64, 711–3. <https://doi.org/10.1055/s-2006-957563>

Eloff, J.N., 1998. A sensitive and quick microplate method to determine the minimal inhibitory concentration of plant extracts for bacteria. *Planta Med.* 64, 711–713. <https://doi.org/10.1055/s-2006-957563>

Emms, D.M., Kelly, S., 2019. OrthoFinder: phylogenetic orthology inference for comparative genomics. *Genome Biol.* 20, 238. <https://doi.org/10.1186/s13059-019-1832-y>

Evans, A., Kavanagh, K.A., 2021. Evaluation of metal-based antimicrobial compounds for the treatment of bacterial pathogens. *J. Med. Microbiol.* 70, 001363. <https://doi.org/10.1099/jmm.0.001363>

Frei, A., Ramu, S., Lowe, G.J., Dinh, H., Semeneć, L., Elliott, A.G., Zuegg, J., Deckers, A., Jung, N., Bräse, S., Cain, A.K., Blaskovich, M.A.T., 2021. Platinum Cyclooctadiene Complexes with Activity against Gram-positive Bacteria. *ChemMedChem* 16, 3165–3171. <https://doi.org/10.1002/cmdc.202100157>

Frei, A., Verderosa, A.D., Elliott, A.G., Zuegg, J., Blaskovich, M.A.T., 2023. Metals to combat antimicrobial resistance. *Nat. Rev. Chem.* 7, 202–224. <https://doi.org/10.1038/s41570-023-00463-4>

Fu, J., Zhang, Y., Lin, S., Zhang, W., Shu, G., Lin, J., Li, H., Xu, F., Tang, H., Peng, G., Zhao, L., Chen, S., Fu, H., 2021. Strategies for Interfering With Bacterial Early Stage Biofilms. *Front. Microbiol.* 12.

Gajic, I., Kabic, J., Kekic, D., Jovicevic, M., Milenkovic, M., Mitic Culafic, D., Trudic, A., Ranin, L., Opavski, N., 2022. Antimicrobial Susceptibility Testing: A Comprehensive Review of Currently Used Methods. *Antibiotics* 11, 427. <https://doi.org/10.3390/antibiotics11040427>

Gemba M, Rosiak E, Nowak-Życzyńska Z, Kałęcka P, Łodykowska E, Kołożyn-Krajewska D. Factors Influencing Biofilm Formation by *Salmonella enterica* sv. *Typhimurium*, *E. cloacae*, *E. hormaechei*, *Pantoea* spp., and *Bacillus* spp. Isolated from Human Milk Determined by PCA Analysis. *Foods*. 2022 Nov 30;11(23):3862. doi: 10.3390/foods11233862. PMID: 36496670; PMCID: PMC9738827.

Ghosh, A., Jayaraman, N., Chatterji, D., 2020. Small-Molecule Inhibition of Bacterial Biofilm. *ACS Omega* 5, 3108–3115. <https://doi.org/10.1021/acsomega.9b03695>

Gu, C.T., Li, C.Y., Yang, L.J., Huo, G.C., 2014. *Enterobacter xiangfangensis* sp. nov., isolated from Chinese traditional sourdough, and reclassification of *Enterobacter sacchari* Zhu et al. 2013 as *Kosakonia sacchari* comb. nov. *Int. J. Syst. Evol. Microbiol.* 64, 2650–2656. <https://doi.org/10.1099/ijs.0.064709-0>

- Gupta, A., Phung, L.T., Taylor, D.E., Silver, S., 2001. Diversity of silver resistance genes in IncH incompatibility group plasmids. *Microbiol. Read. Engl.* 147, 3393–3402. <https://doi.org/10.1099/00221287-147-12-3393>
- Ho, N.R., Kondiah, K., De Maayer, P., 2018a. Complete Genome Sequence of *Enterobacter xiangfangensis* Pb204, a South African Strain Capable of Synthesizing Gold Nanoparticles. *Microbiol. Resour. Announc.* 7, e01406-18. <https://doi.org/10.1128/MRA.01406-18>
- Huerta-Cepas, J., Forslund, K., Coelho, L.P., Szklarczyk, D., Jensen, L.J., von Mering, C., Bork, P., 2017. Fast Genome-Wide Functional Annotation through Orthology Assignment by eggNOG-Mapper. *Mol. Biol. Evol.* 34, 2115–2122. <https://doi.org/10.1093/molbev/msx148>
- Inweregbu, K., Dave, J., Pittard, A., 2005. Nosocomial infections. *Contin. Educ. Anaesth. Crit. Care Pain* 5, 14–17. <https://doi.org/10.1093/bjaceaccp/mki006>
- Karlowsky, J.A., Hoban, D.J., Hackel, M.A., Lob, S.H., Sahm, D.F., 2017. Resistance among Gram-negative ESKAPE pathogens isolated from hospitalized patients with intra-abdominal and urinary tract infections in Latin American countries: SMART 2013-2015. *Braz. J. Infect. Dis.* 21, 343–348. <https://doi.org/10.1016/j.bjid.2017.03.006>
- Khan, H.A., Baig, F.K., Mehboob, R., 2017. Nosocomial infections: Epidemiology, prevention, control and surveillance. *Asian Pac. J. Trop. Biomed.* 7, 478–482. <https://doi.org/10.1016/j.apjtb.2017.01.019>
- Khan, Z.A., Siddiqui, M.F., Park, S., 2019. Current and Emerging Methods of Antibiotic Susceptibility Testing. *Diagnostics* 9, 49. <https://doi.org/10.3390/diagnostics9020049>
- Kishen, A., Haapasalo, M., 2010. Biofilm models and methods of biofilm assessment. *Endod. Top.* 22, 58–78. <https://doi.org/10.1111/j.1601-1546.2012.00285.x>
- Klančnik, A., Piskernik, S., Jeršek, B., Možina, S.S., 2010. Evaluation of diffusion and dilution methods to determine the antibacterial activity of plant extracts. *J. Microbiol. Methods* 81, 121–126. <https://doi.org/10.1016/j.mimet.2010.02.004>
- Koban, I., Matthes, R., Hübner, N.-O., Welk, A., Sietmann, R., Lademann, J., Kramer, A., Kocher, T., 2012. XTT assay of ex-vivo saliva biofilms to test antimicrobial

influences. GMS Krankenhaushygiene Interdiszip. 7, Doc06.
<https://doi.org/10.3205/dgkh000190>

Konop, M., Damps, T., Misicka, A., Rudnicka, L., 2016. Certain aspects of silver and silver nanoparticles in wound care: a minireview. J. Nanomater. 2016, 47:47.
<https://doi.org/10.1155/2016/7614753>

Kowalska-Krochmal, B., Dudek-Wicher, R., 2021. The Minimum Inhibitory Concentration of Antibiotics: Methods, Interpretation, Clinical Relevance. Pathogens 10, 165. <https://doi.org/10.3390/pathogens10020165>

Kralik, P., Ricchi, M., 2017. A Basic Guide to Real Time PCR in Microbial Diagnostics: Definitions, Parameters, and Everything. Front. Microbiol. 8.

Li, R., Chen, J., Cesario, T.C., Wang, X., Yuan, J.S., Rentzepis, P.M., 2016. Synergistic reaction of silver nitrate, silver nanoparticles, and methylene blue against bacteria. Proc. Natl. Acad. Sci. 113, 13612–13617.
<https://doi.org/10.1073/pnas.1611193113>

Liu, S., Chen, L., Wang, L., Zhou, B., Ye, D., Zheng, X., Lin, Y., Zeng, W., Zhou, T., Ye, J., 2022. Cluster Differences in Antibiotic Resistance, Biofilm Formation, Mobility, and Virulence of Clinical Enterobacter cloacae Complex. Front. Microbiol. 13, 814831.
<https://doi.org/10.3389/fmicb.2022.814831>

Liu, W.-Y., Wong, C.-F., Chung, K.M.-K., Jiang, J.-W., Leung, F.C.-C., 2013. Comparative Genome Analysis of Enterobacter cloacae. PLOS ONE 8, e74487.
<https://doi.org/10.1371/journal.pone.0074487>

Llaca-Díaz, J.M., Mendoza-Olazarán, S., Camacho-Ortiz, A., Flores, S., Garza-González, E., 2012. One-Year Surveillance of ESKAPE Pathogens in an Intensive Care Unit of Monterrey, Mexico. Chemotherapy 58, 475–481.
<https://doi.org/10.1159/000346352>

Lok, C.-N., Ho, C.-M., Chen, R., Tam, P.K.-H., Chiu, J.-F., Che, C.-M., 2008. Proteomic identification of the Cus system as a major determinant of constitutive *Escherichia coli* silver resistance of chromosomal origin. J. Proteome Res. 7, 2351–2356. <https://doi.org/10.1021/pr700646b>

Lowman, W., 2016. Active surveillance of hospital-acquired infections in South Africa: Implementation, impact and challenges. *S. Afr. Med. J.* 106, 489–493. <https://doi.org/10.7196/SAMJ.2016.v106i5.10783>

Ma, Y., Wang, C., Li, Y., Li, J., Wan, Q., Chen, J., Tay, F.R., Niu, L., 2020. Considerations and Caveats in Combating ESKAPE Pathogens against Nosocomial Infections. *Adv. Sci.* 7, 1901872. <https://doi.org/10.1002/advs.201901872>

Medici, S., Peana, M., Crisponi, G., Nurchi, V.M., Lachowicz, J.I., Remelli, M., Zoroddu, M.A., 2016. Silver coordination compounds: A new horizon in medicine. *Coord. Chem. Rev.*, A Special Issue in Honor of Professor Henryk Kozłowski 327–328, 349–359. <https://doi.org/10.1016/j.ccr.2016.05.015>

Medici, S., Peana, M., Nurchi, V.M., Zoroddu, M.A., 2019. Medical Uses of Silver: History, Myths, and Scientific Evidence. *J. Med. Chem.* 62, 5923–5943. <https://doi.org/10.1021/acs.jmedchem.8b01439>

Mezzatesta, M.L., Gona, F., Stefani, S., 2012. *Enterobacter cloacae* complex: clinical impact and emerging antibiotic resistance. *Future Microbiol.* 7, 887–902. <https://doi.org/10.2217/fmb.12.61>

Miškovská, A., Rabochová, M., Michailidu, J., Masák, J., Čejková, A., Lorinčík, J., Mařátková, O., 2022. Antibiofilm activity of silver nanoparticles biosynthesized using viticultural waste. *PLoS ONE* 17, e0272844. <https://doi.org/10.1371/journal.pone.0272844>

Misra, T., Tare, M., Jha, P.N., 2022. Insights Into the Dynamics and Composition of Biofilm Formed by Environmental Isolate of *Enterobacter cloacae*. *Front. Microbiol.* 13.

Morones-Ramirez, J.R., Winkler, J.A., Spina, C.S., Collins, J.J., 2013. Silver Enhances Antibiotic Activity Against Gram-negative Bacteria. *Sci. Transl. Med.* 5, 190ra81. <https://doi.org/10.1126/scitranslmed.3006276>

Muhammad, M.H., Idris, A.L., Fan, X., Guo, Y., Yu, Y., Jin, X., Qiu, J., Guan, X., Huang, T., 2020. Beyond Risk: Bacterial Biofilms and Their Regulating Approaches. *Front. Microbiol.* 11.

Mustafa, A., Ibrahim, M., Rasheed, M.A., Kanwal, S., Hussain, A., Sami, A., Ahmed, R., Bo, Z., 2020. Genome-wide Analysis of Four *Enterobacter cloacae* complex type

strains: Insights into Virulence and Niche Adaptation. *Sci. Rep.* 10, 8150. <https://doi.org/10.1038/s41598-020-65001-4>

Nikaido, H., 2009. Multidrug Resistance in Bacteria. *Annu. Rev. Biochem.* 78, 119–146. <https://doi.org/10.1146/annurev.biochem.78.082907.145923>

Oaks, R.J., Cindass, R., 2023. Silver Sulfadiazine, in: *StatPearls*. StatPearls Publishing, Treasure Island (FL).

Oliveira, D.M.P.D., Forde, B.M., Kidd, T.J., Harris, P.N.A., Schembri, M.A., Beatson, S.A., Paterson, D.L., Walker, M.J., 2020. Antimicrobial Resistance in ESKAPE Pathogens. *Clin. Microbiol. Rev.* <https://doi.org/10.1128/CMR.00181-19>

Olivier, C., Kunneke, H., O'Connell, N., von Delft, E., Wates, M., Dramowski, A., 2018. Healthcare-associated infections in paediatric and neonatal wards: A point prevalence survey at four South African hospitals. *SAMJ South Afr. Med. J.* 108, 418–422. <https://doi.org/10.7196/samj.2018.v108i5.12862>

Ortego, L., Gonzalo-Asensio, J., Laguna, A., Villacampa, M.D., Gimeno, M.C., 2015a. (Aminophosphane)gold(I) and silver(I) complexes as antibacterial agents. *J. Inorg. Biochem.* 146, 19–27. <https://doi.org/10.1016/j.jinorgbio.2015.01.007>

O'Shaughnessy, M., McCarron, P., Viganor, L., McCann, M., Devereux, M., Howe, O., 2020. The Antibacterial and Anti-Biofilm Activity of Metal Complexes Incorporating 3,6,9-Trioxaundecanedioate and 1,10-Phenanthroline Ligands in Clinical Isolates of *Pseudomonas aeruginosa* from Irish Cystic Fibrosis Patients. *Antibiotics* 9, 674. <https://doi.org/10.3390/antibiotics9100674>

Oun, R., Moussa, Y.E., Wheate, N.J., 2018. The side effects of platinum-based chemotherapy drugs: a review for chemists. *Dalton Trans. Camb. Engl.* 2003 47, 6645–6653. <https://doi.org/10.1039/c8dt00838h>

Overbeek, R., Olson, R., Pusch, G.D., Olsen, G.J., Davis, J.J., Disz, T., Edwards, R.A., Gerdes, S., Parrello, B., Shukla, M., Vonstein, V., Wattam, A.R., Xia, F., Stevens, R., 2014. The SEED and the Rapid Annotation of microbial genomes using Subsystems Technology (RAST). *Nucleic Acids Res.* 42, D206-214. <https://doi.org/10.1093/nar/gkt1226>

Pankey, G.A., Sabath, L.D., 2004. Clinical Relevance of Bacteriostatic versus Bactericidal Mechanisms of Action in the Treatment of Gram-Positive Bacterial Infections. *Clin. Infect. Dis.* 38, 864–870. <https://doi.org/10.1086/381972>

Patil, A., Banerji, R., Kanojiya, P., Saroj, S.D., n.d. Foodborne ESKAPE Biofilms and Antimicrobial Resistance: lessons Learned from Clinical Isolates. *Pathog. Glob. Health* 115, 339–356. <https://doi.org/10.1080/20477724.2021.1916158>

Pipattanachat, S., Qin, J., Rokaya, D., Thanyasrisung, P., Srimaneepong, V., 2021. Biofilm inhibition and bactericidal activity of NiTi alloy coated with graphene oxide/silver nanoparticles via electrophoretic deposition. *Sci. Rep.* 11, 14008. <https://doi.org/10.1038/s41598-021-92340-7>

Politano, A.D., Campbell, K.T., Rosenberger, L.H., Sawyer, R.G., 2013. Use of Silver in the Prevention and Treatment of Infections: Silver Review. *Surg. Infect.* 14, 8–20. <https://doi.org/10.1089/sur.2011.097>

Poole, K., 2007. Efflux pumps as antimicrobial resistance mechanisms. *Ann. Med.* 39, 162–176. <https://doi.org/10.1080/07853890701195262>

Pourhajibagher M, Chiniforush, N, Shahabi, S, Ghorbanzadeh, R, Bahador, A, 2016. Sub-lethal doses of photodynamic therapy affect biofilm formation ability and metabolic activity of *Enterococcus faecalis*, *Photodiagnosis and Photodynamic Therapy*, Volume 15, <https://doi.org/10.1016/j.pdpdt.2016.06.003>.

Prakash, B., Veeregowda, B.M., Krishnappa, G., 2003. Biofilms: A survival strategy of bacteria. *Curr. Sci.* 85, 1299–1307.

Pricker, S.P., 1996. Medical uses of gold compounds: Past, present and future. *Gold Bull.* 29, 53–60. <https://doi.org/10.1007/BF03215464>

Ramsamy, Y., Essack, S.Y., Sartorius, B., Patel, M., Mlisana, K.P., 2018. Antibiotic resistance trends of ESKAPE pathogens in Kwazulu-Natal, South Africa: A five-year retrospective analysis. *Afr. J. Lab. Med.* 7. <https://doi.org/10.4102/ajlm.v7i2.887>

Randall, C.P., Gupta, A., Jackson, N., Busse, D., O'Neill, A.J., 2015. Silver resistance in Gram-negative bacteria: a dissection of endogenous and exogenous mechanisms. *J. Antimicrob. Chemother.* 70, 1037–1046. <https://doi.org/10.1093/jac/dku523>

Ratia, C., Cepas, V., Soengas, R., Navarro, Y., Velasco-de Andrés, M., Iglesias, M.J., Lozano, F., López-Ortiz, F., Soto, S.M., 2022. A C₄S-Cyclometallated Gold(III) Complex as a Novel Antibacterial Candidate Against Drug-Resistant Bacteria. *Front. Microbiol.* 13, 815622. <https://doi.org/10.3389/fmicb.2022.815622>

Reller, L.B., Weinstein, M., Jorgensen, J.H., Ferraro, M.J., 2009. Antimicrobial Susceptibility Testing: A Review of General Principles and Contemporary Practices. *Clin. Infect. Dis.* 49, 1749–1755. <https://doi.org/10.1086/647952>

Ruhal, R., Kataria, R., 2021. Biofilm patterns in Gram-positive and Gram-negative bacteria. *Microbiol. Res.* 251, 126829. <https://doi.org/10.1016/j.micres.2021.126829>

Santajit, S., Indrawattana, N., 2016. Mechanisms of Antimicrobial Resistance in ESKAPE Pathogens. *BioMed Res. Int.* 2016, 1–8. <https://doi.org/10.1155/2016/2475067>

Scherbaum, M., Kösters, K., Mürbeth, R.E., Ngoa, U.A., Kremsner, P.G., Lell, B., Alabi, A., 2014. Incidence, pathogens and resistance patterns of nosocomial infections at a rural hospital in Gabon. *BMC Infect. Dis.* 14, 124. <https://doi.org/10.1186/1471-2334-14-124>

Selem, E., Mekky, A.F., Hassanein, W.A., Reda, F.M., Selim, Y.A., 2022. Antibacterial and antibiofilm effects of silver nanoparticles against the uropathogen *Escherichia coli* U12. *Saudi J. Biol. Sci.* 29, 103457. <https://doi.org/10.1016/j.sjbs.2022.103457>

Shamaila, S., Zafar, N., Riaz, S., Sharif, R., Nazir, J., Naseem, S., 2016. Gold Nanoparticles: An Efficient Antimicrobial Agent against Enteric Bacterial Human Pathogen. *Nanomaterials* 6, 71. <https://doi.org/10.3390/nano6040071>

Sharma, D., Misba, L., Khan, A.U., 2019. Antibiotics versus biofilm: an emerging battleground in microbial communities. *Antimicrob. Resist. Infect. Control* 8, 76. <https://doi.org/10.1186/s13756-019-0533-3>

Siddique, M.H., Aslam, B., Imran, M., Ashaf, A., Nadeem, H., Hayat, S., Khurshid, M., Afzal, M., Malik, I.R., Shahzad, M., Qureshi, U., Khan, Z.U.H., Muzammil, S., 2020. Effect of Silver Nanoparticles on Biofilm Formation and EPS Production of Multidrug-Resistant *Klebsiella pneumoniae*. *BioMed Res. Int.* 2020, 6398165. <https://doi.org/10.1155/2020/6398165>

Sikora, A., Zaha, F., 2022. Nosocomial Infections, in: StatPearls. StatPearls Publishing, Treasure Island (FL).

Silver, S., 2003. Bacterial silver resistance: molecular biology and uses and misuses of silver compounds. *FEMS Microbiol. Rev.* 27, 341–353. [https://doi.org/10.1016/S0168-6445\(03\)00047-0](https://doi.org/10.1016/S0168-6445(03)00047-0)

Sivashankari, S., Shanmughavel, P., 2007. Comparative genomics - A perspective. *Bioinformatics* 1, 376–378.

Song, Y.J., Yu, H.H., Kim, Y.J., Paik, N.-K.L. and H.-D., 2019. Anti-Biofilm Activity of Grapefruit Seed Extract against *Staphylococcus aureus* and *Escherichia coli* 29, 1177–1183. <https://doi.org/10.4014/jmb.1905.05022>

Teh, C.H., Nazni, W.A., Nurulhusna, A.H., Norazah, A., Lee, H.L., 2017. Determination of antibacterial activity and minimum inhibitory concentration of larval extract of fly via resazurin-based turbidometric assay. *BMC Microbiol.* 17, 36. <https://doi.org/10.1186/s12866-017-0936-3>

Turner, R.J., 2017. Metal-based antimicrobial strategies. *Microb. Biotechnol.* 10, 1062–1065. <https://doi.org/10.1111/1751-7915.12785>

Tuttobene, M.R., Pérez, J.F., Pavesi, E.S., Perez Mora, B., Biancotti, D., Cribb, P., Altilio, M., Müller, G.L., Gramajo, H., Tamagno, G., Ramírez, M.S., Diacovich, L., Mussi, M.A., 2021. Light Modulates Important Pathogenic Determinants and Virulence in ESKAPE Pathogens *Acinetobacter baumannii*, *Pseudomonas aeruginosa*, and *Staphylococcus aureus*. *J. Bacteriol.* 203. <https://doi.org/10.1128/JB.00566-20>

van Vliet, A.H.M., Bereswill, S., Kusters, J.G., 2001. Ion Metabolism and Transport, in: Mobley, H.L., Mendz, G.L., Hazell, S.L. (Eds.), *Helicobacter pylori: Physiology and Genetics*. ASM Press, Washington (DC).

Vestby, L.K., Grønseth, T., Simm, R., Nesse, L.L., 2020. Bacterial Biofilm and its Role in the Pathogenesis of Disease. *Antibiotics* 9, 59. <https://doi.org/10.3390/antibiotics9020059>

Vivas, R., Barbosa, A.A.T., Dolabela, S.S., Jain, S., 2019. Multidrug-Resistant Bacteria and Alternative Methods to Control Them: An Overview. *Microb. Drug Resist.* 25, 890–908. <https://doi.org/10.1089/mdr.2018.0319>

- Wang, H., Li, Jia, Min, C., Xia, F., Tang, M., Li, Jun, Hu, Y., Zou, M., 2022. Characterization of Silver Resistance and Coexistence of sil Operon with Antibiotic Resistance Genes Among Gram-Negative Pathogens Isolated from Wound Samples by Using Whole-Genome Sequencing. *Infect. Drug Resist.* 15, 1425–1437. <https://doi.org/10.2147/IDR.S358730>
- Wang, H.-H., Su, C.-H., Wu, Y.-J., Lin, C.-A.J., Lee, C.-H., Shen, J.-L., Chan, W.-H., Chang, W.H., Yeh, H.-I., 2012. Application of Gold in Biomedicine: Past, Present and Future. *Int. J. Gerontol.* 6, 1–4. <https://doi.org/10.1016/j.ijge.2011.09.015>
- Wang, Y., Wan, J., Miron, R.J., Zhao, Y., Zhang, Y., 2016. Antibacterial properties and mechanisms of gold-silver nanocages. *Nanoscale* 8, 11143–11152. <https://doi.org/10.1039/c6nr01114d>
- Webber, M.A., Piddock, L.J.V., 2003. The importance of efflux pumps in bacterial antibiotic resistance. *J. Antimicrob. Chemother.* 51, 9–11. <https://doi.org/10.1093/jac/dkg050>
- Wilson, B.M., Chakhtoura, N.G.E., Patel, S., Saade, E., Donskey, C.J., Bonomo, R.A., Perez, F., n.d. Carbapenem-Resistant *Enterobacter cloacae* in Patients from the US Veterans Health Administration, 2006–2015 - Volume 23, Number 5—May 2017 - Emerging Infectious Diseases journal - CDC. <https://doi.org/10.3201/eid2305.162034>
- Wilson, C., Lukowicz, R., Merchant, S., Valquier-Flynn, H., Caballero, J., Sandoval, J., Okuom, M., Huber, C., Brooks, T.D., Wilson, E., Clement, B., Wentworth, C.D., Holmes, A.E., 2017. Quantitative and Qualitative Assessment Methods for Biofilm Growth: A Mini-review. *Res. Rev. J. Eng. Technol.* 6, <http://www.rroj.com/open-access/quantitative-and-qualitative-assessment-methods-for-biofilm-growth-a-minireview-.pdf>.
- Wu, B., Yang, X., Yan, M., 2019. Synthesis and Structure-Activity Relationship Study of Antimicrobial Auranofin against ESKAPE Pathogens. *J. Med. Chem.* 62, 7751–7768. <https://doi.org/10.1021/acs.jmedchem.9b00550>
- Wu, J., Li, F., Hu, X., Lu, J., Sun, X., Gao, J., Ling, D., 2019. Responsive Assembly of Silver Nanoclusters with a Biofilm Locally Amplified Bactericidal Effect to Enhance Treatments against Multi-Drug-Resistant Bacterial Infections. *ACS Cent. Sci.* 5, 1366–1376. <https://doi.org/10.1021/acscentsci.9b00359>

Xu, Z., Liang, Y., Lin, S., Chen, D., Li, B., Li, L., Deng, Y., 2016. Crystal Violet and XTT Assays on *Staphylococcus aureus* Biofilm Quantification. *Curr. Microbiol.* 73, 474–482. <https://doi.org/10.1007/s00284-016-1081-1>

Yang, X., Ye, W., Qi, Y., Ying, Y., Xia, Z., 2021. Overcoming Multidrug Resistance in Bacteria Through Antibiotics Delivery in Surface-Engineered Nano-Cargos: Recent Developments for Future Nano-Antibiotics. *Front. Bioeng. Biotechnol.* 9.

APPENDIX A

A1.1 CHARACTERIZATION OF COMPOUNDS

The study explored eight distinct silver(I) phosphine compounds, namely, UJ1 (Barron *et al.*, 1986; Berners Price and Sadler, 1988; Jenkins, 2014; Ferreira, 2023), UJ2 (Engelbrecht, 2017), UJ3 (Ferreira *et al.*, 2015, Engelbrecht *et al.*, 2018a), UJ4 (Engelbrecht, 2017), UJ1A (Engelbrecht, 2017), UJ15 (Engelbrecht, 2017), UJ34 (Barron *et al.*, 1986, Engelbrecht *et al.*, 2018b) and UJ35 (Ferreria *et al.*, 2015; Human *et al.*, 2015) of which their synthesis is described elsewhere. Since multiple batches of these complexes were made, using the same methods, only the characterization of the specific batch used (where applicable) is included in this study. For this purpose, the melting points were determined using a Stuart Scientific Melting Point apparatus SMP10 and left uncorrected. The infrared (IR) spectrum was measured and recorded on a Bruker Tensor 27 FT-IR spectrophotometer, using an attenuated total reflectance (ATR) accessory with a diamond crystal. Nuclear magnetic resonance (NMR) spectra using the following isotopes: ^1H NMR (400 MHz), ^{13}C NMR (75 MHz) and ^{31}P NMR (161 MHz) were measured and recorded on a BrukerAvance III 400 MHz spectrometer. NMR data was referenced to a tetramethylsilane (TMS) internal standard using residual protonated impurities in the deuterated chloroform (CDCl_3) solvent. Microanalysis (i.e. elemental analysis or EA) was performed by Dr Edith Antunes in the Department of Chemistry, Rhodes University on a Thermo Flash 2000 series CHNS/O Organic Elemental Analyzer.

Synthesis of UJ1: Silver(I) bromide triphenylphosphine [AgBr {(PPh₃)₃}] - batch A21

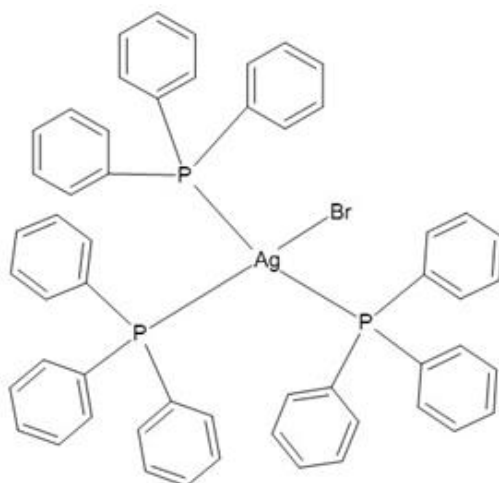


Figure A1.1: Chemical structure of **UJ1** (Jenkins, 2014, Ferreira, 2023).

Melting point: 160-162°C.

IR (Solid): ν_{\max} (cm⁻¹): 3046.66(v (=C-H), w), 2576.80 (v (alkane, C-H, stretch), asymm, w), 1885.23, 1667.24, 1584.25 (v (C=C aromatic), m), 1477.26, 1432.35 (v (C=C aromatic), m), 1382.60 (s), 1328.19, 1306.82 (s), 1180.90-841.85 (v (aromatic, C-H bend, meta), s), 749.51, 739.62690.76 (v (aromatic, C-H bend, ortho),m).

¹H NMR (CDCl₃, 400 MHz) δ (ppm): 7.371-7.185 (m, 45H, Ar-H).

¹³C NMR (CDCl₃, 100 MHz) δ (ppm): 134.03 (d), 132.59 (d), 129.96 (s), 128.75 (d, aromatic carbon).

³¹P NMR (161 MHz, CDCl₃) δ (ppm): 5.03 (single peak)

Elemental analysis: C₅₄H₄₅AgBrP₃: Calculated: C, 66.55%; H, 4.65%. Found: C, 66.12%; H, 4.45%.

Synthesis of UJ2: Silver(I) chloride tris(4-chlorophenyl) phosphine [AgCl{(pClC₆H₄)₃P}₃] - batch A31

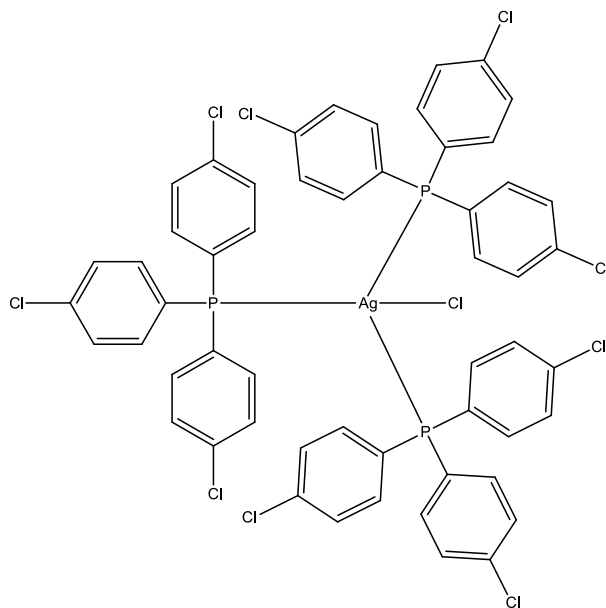


Figure A1.2: Chemical structure of **UJ2** (Engelbrecht, 2017; Mizan, 2023).

Melting Point: 261-262°C.

IR (Solid): ν_{\max} (cm⁻¹): 3050.33(v (=C-H), w), 1574.10, 1560.49 (v (C=C aromatic), m), 1180.13 (s), 1079.06-812.18 (v (aromatic, C-H bend, meta), s), 744.07, 703.67 (v (aromatic, C-H bend, ortho),m).

¹H NMR (CDCl₃, 400 MHz) δ (ppm): 7.281-7.183 (m, 36H, Ar-H).

¹³C-NMR (CDCl₃, 100 MHz) δ (ppm): 136.73 (s), 134.94 (d), 131.4 (d), 129.21 (d, aromatic carbon)

³¹P NMR (CDCl₃, 161 MHz) δ (ppm): -0.96 (single peak)

Elemental analysis: C₅₄H₃₆AgCl₁₀P₃: Calculated: C, 52.3%; H, 2.93%. Found: C, 52.12%; H, 2.83%.

Synthesis of UJ3: Silver(I) thiocyanate 4-methoxyphenyl phosphine [AgSCN{P(4-MeOC6H4)3}2]2 – batch A64

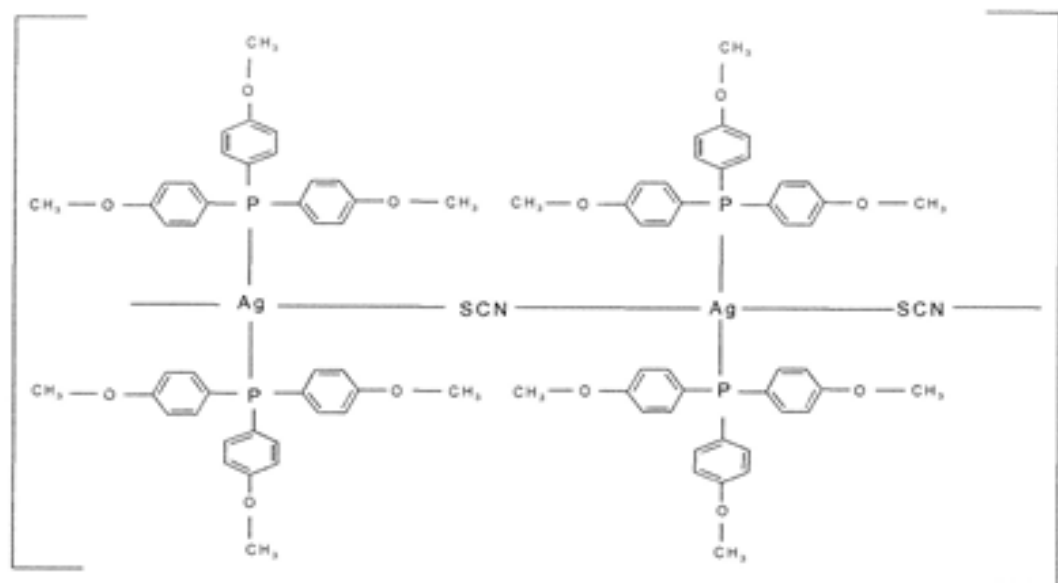


Figure A1.3: Chemical structure of **UJ3** (Ferreira *et al.*, 2015; Engelbrecht *et al.*, 2018)

Melting point: 204-206°C.

IR (Solid): ν_{\max} (cm^{-1}): 2957.86, 2836.19, 2361.43 (v(alkane, C-H. stretch), asymm, w) 2080.97 (v(SCN), m); 1736.16 (w); 1591.67, 1568.12 (v(C=C aromatic), asymm, s); 1496.86, 1458.16, 1440.31 (asymm) 1404.06 (v(C=C aromatic), s, m);, 1289.63, 1247.26, 1176.17 (v(OCH₃), s); 1098.03(s), 1024.70 (s); 822.09, 797.13 (v(aromatic, δ C-H para), asymm, s); 716 (v(aromatic, δ C-H mono), asymm, s); 656.07, 637.51(v(aromatic, δ C-H meta), asymm, m).

¹H NMR (CDCl₃, 400 MHz) δ (ppm): 2.96 (s, 18H, OCH₃), 7.280-6.601 (m, 25H, Ar-H)

¹³C-NMR (CDCl₃, 100 MHz) δ (ppm): 161.11 (s), 135.21 (d), 123.68 (d), 114.50 (d, aromatic carbon).; 55.24 (s, OCH₃)

³¹P NMR (CDCl₃, 161 MHz) δ (ppm): 5.31 (single peak)

Elemental analysis: C₄₃H₄₂AgNO₆SP₂: Calculated: C, 59.32%; H, 4.86% Found: C, 59.29%; H, 4.56%

Synthesis of UJ4: Silver(I) nitrate tris(4-chlorophenyl) phosphine [AgNO₃ {(pClC₆H₄)₃P}₃] - batch A42

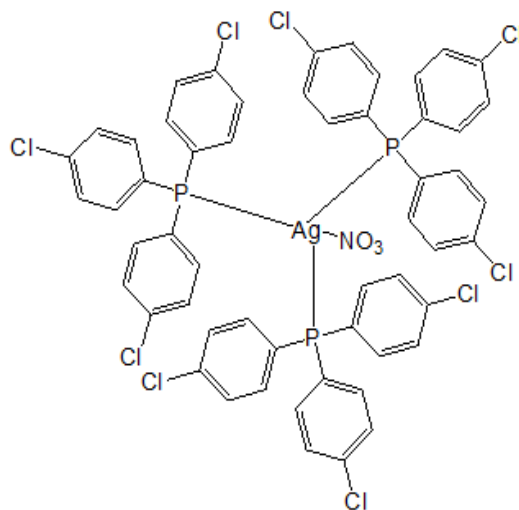


Figure A1.4: Chemical structure of **UJ4** (Engelbrecht, 2017)

Melting point: 170-172°C.

IR (Solid): ν_{\max} (cm⁻¹): 3061.70 (v (=C-H), w), 1977.03, 1729.28 (v (alkane, C-H, stretch), asymm, w), 1575.44, 1575.44, 1561.78 (v (C=C aromatic), m), 1479.35, 1405.36, 1385.10, 1298.25 (v (C=C aromatic), m), 1180.55-812.11 (v (aromatic, C-H bend, meta), s), 745.25, 704.25, 557.90, 534.24 (v (aromatic, C-H bend, ortho), m).

¹H NMR (CDCl₃, 400 MHz) δ (ppm): 7.279-7.133 (m, 45H, Ar-H).

¹³C NMR (CDCl₃, 100 MHz) δ (ppm): 137.25 (s); 134.73 (d), 130.42 (d), 129.46 (d, aromatic carbon).

³¹P NMR (161 MHz, CDCl₃) δ (ppm): 3.45 (single peak)

Elemental analysis: C₅₄H₃₆AgCl₉NO₃P₃: Calculated: C, 51.20%; H, 2.86%. Found: C, 51.00%; H, 2.62%.

Synthesis of UJ1A: Silver(I) bromide tri(*p*-tolyl)phosphine [AgBr(4-CH₃PPh₃)₃] - batch A45

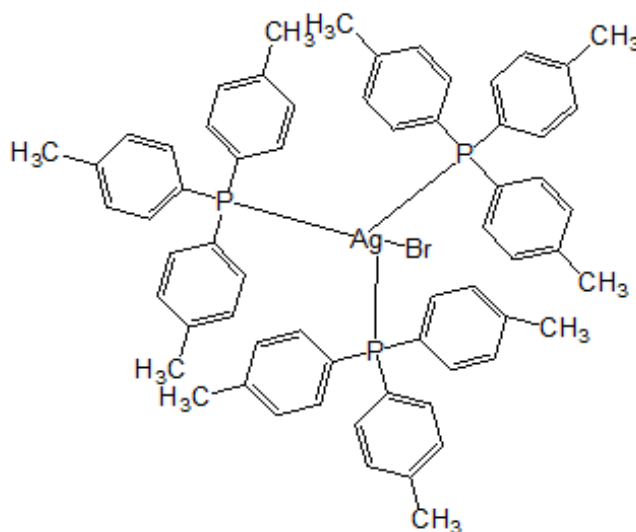


Figure A1.5:
structure of **UJ1A** (Engelbrecht, 2017)

Chemical

Melting point: 224-226°C.

IR (Solid): ν_{\max} (cm⁻¹): 3017.86, 2918.52 (ν (=C-H), w), 2140.60, 2024.24 (ν (alkane, C-H, stretch), asymm, w), 1908.55 (w), 1807.71 (s), 1647.99, 1597.43, 1560.32 (ν (C=C aromatic), m), 1497.66, 1446.44 (ν (C=C aromatic), m), 1396.08 (ν (CH₃ bend), m), 1379.59 (w), 1307.24, 1271.94 (s), 1214.04 (w), 1188.05-805.00.64 (ν (aromatic, C-H bend, meta), s), 710.08, 641.95, 628.71, 609.33 (ν (aromatic, C-H bend, ortho),m).

¹H NMR (CDCl₃, 400 MHz) δ (ppm): 2.346 (s, 27H, CH₃), 7.265-7.055 (m, 36H, Ar-H).

¹³C NMR (CDCl₃, 100 MHz) δ (ppm): 139.52 (s), 133.84 (d), 130.74 (d), 129.32 (d, aromatic carbon), 21.39 (s, CH₃),

³¹P NMR (161 MHz, CDCl₃) δ (ppm): 0.70 (single peak)

Elemental analysis: C₆₃H₆₃AgBrP₃: Calculated: C, 68.73%; H, 5.77%. Found: C, 68.70%; H, 5.55%.

Synthesis of UJ15: Silver(I) nitrate tri(p-tolyl)phosphine [AgNO₃(4-CH₃PPh₃)₃]

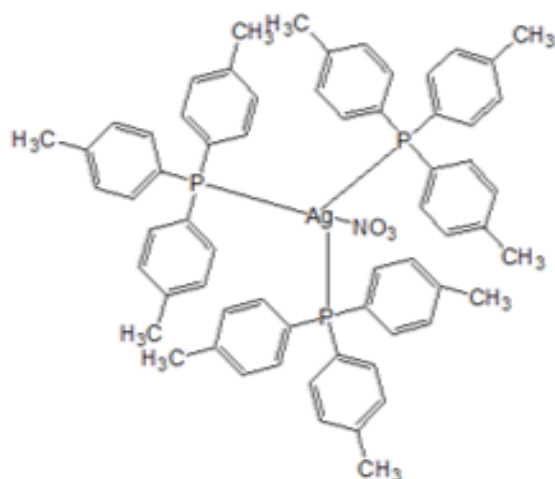


Figure A1.6: Chemical structure of **UJ15** (Engelbrecht, 2017)

The characterization of this batch is reported elsewhere (Engelbrecht, 2017)

Synthesis of UJ34: Silver(I) nitrate triphenylphosphine [AgNO₃(PPh₃)₂] – batch A18

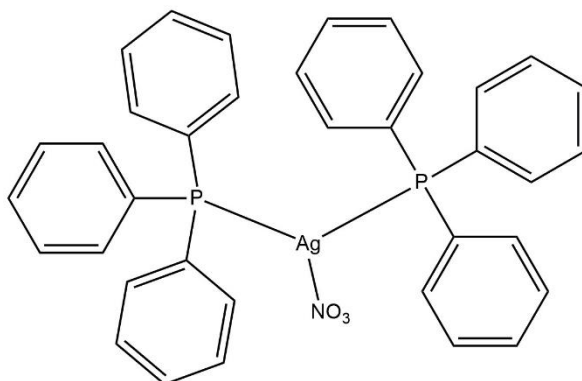


Figure A1.7: Chemical structure of **UJ34** (Engelbrecht *et al.*,2018b)

Melting point: 220-222°C.

IR (Solid): ν_{\max} (cm⁻¹): 3046.26 (v (=C-H), w), 2348.67 (v (alkane, C-H, stretch), asym, w), 1584.18, 1471.54, 1433.75 (C=C aromatic), m), 1315.71 (s), 1285.23, 1184.32-846.54 (v (aromatic, C-H bend, meta), s), 741.12, 691.58 (v (aromatic, C-H bend, ortho),m).

¹H NMR (CDCl₃, 400 MHz) δ (ppm): 7.291-1.101 (m, 30H, Ar-H).

¹³C NMR (CDCl₃, 100 MHz) δ (ppm): 134.02 (d), 133.46 (d), 129.60 (s), 128.59 (d, aromatic carbon)

³¹P NMR (161 MHz, CDCl₃) δ (ppm): 2.30 (single peak)

Elemental analysis: C₃₆H₃₀AgNO₃P₂: Calculated: C, 62.26%; H, 4.35%. Found: C, 62.20%; H, 4.46%.

Synthesis of UJ35: Silver(I) thiocyanide tris(4-chlorophenyl) phosphine [AgSCN(pClC₆H₄)₃P]₂ - batch A28

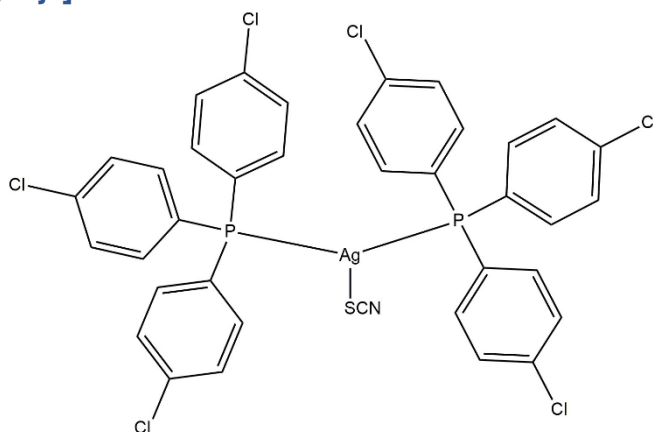


Figure A1.8: Chemical structure of **UJ35** (Ferreria *et al.*, 2015; Human *et al.*, 2015)

Melting point: 240-242°C.

IR (Solid): ν_{\max} (cm⁻¹): 3010.80 (v (=C-H), w), 2878.25, 2155.10 (v (alkane, C-H, stretch), asymm, w), 2077.32 (v (SCN), m), 1704.51 (w), 1574.39 (v (C=C aromatic), m), 1476.52, 1385.87, 1297.57 (v (C=C aromatic), m), , 1097.47-813.54 (v (aromatic, C-H bend, meta), s), 744.06, 704.31 (v (aromatic, C-H bend, ortho), m).

¹H NMR (CDCl₃, 400 MHz) δ (ppm): 7.280-7.208 (m, 24H, Ar-H).

¹³C NMR (CDCl₃, 100 MHz) δ (ppm): 137.04 (s), 134.86 (d), 130.63 (d), 129.36 (d, aromatic carbon)

³¹P NMR (161 MHz, CDCl₃) δ (ppm): 2.76 (single peak)

Elemental analysis: C₃₇H₂₄AgCl₆NP₂S: Calculated: C, 49.53%; H, 2.70%. Found: C, 49.15%; H, 2.61%.

References

- Barron, P.F., Dyason, J.C., Healy, P.C., Engelhardt, L.M., Skelton, B.W., White, A.H. (1986) Lewis base adducts of Group 11 metal compounds. Part 24. Co-ordination of triphenylphosphine with silver nitrate - A solid-state cross-polarization magic angle spinning ^{31}P nuclear magnetic resonance, crystal structure, and infrared spectroscopic study of $\text{Ag}(\text{PPh}_3)_n\text{NO}_3$ ($n= 1-4$), *Journal of Chemistry Society Dalton Transactions*, 1965-1970
- Berners-Price, S.J., Sadler, P.J. (1988) Structure and bonding, phosphine and metal phosphine complexes: Relationship of chemistry to anticancer and other biological activity, *Bioinorganic Chemistry*, 70: 27-102
- Engelbrecht, Z. (2017). Novel anticancer silver (I) phosphines proven to target the mitochondrial-mediated cell death pathway in malignant cells. University of Johannesburg (South Africa).
- Engelbrecht, Z., Meijboom, R. and Cronjé, M.J. (2018a). The ability of silver (I) thiocyanate 4-methoxyphenyl phosphine to induce apoptotic cell death in esophageal cancer cells is correlated to mitochondrial perturbations. *BioMetals*, 31, pp.189-202.
- Engelbrecht, Z., Potgieter, K., Mpela, Z., Malgas-Enus, R., Meijboom, R. and Cronje, M.J. (2018b). A comparison of the toxicity of mono, Bis, Tris and tetrakis phosphino silver complexes on SNO esophageal cancer cells. *Anti-Cancer Agents in Medicinal Chemistry (Formerly Current Medicinal Chemistry-Anti-Cancer Agents)*, 18(3), pp.394-400.
- Ferreira, E., Munyaneza, A., Omondi, B., Meijboom, R. and Cronjé, M.J. (2015). The effect of 1: 2 Ag (I) thiocyanate complexes in MCF-7 breast cancer cells. *Biometals*, 28, pp.765-781.
- Human, Z., Munyaneza, A., Omondi, B., Sanabria, N.M., Meijboom, R. and Cronjé, M.J. (2015). The induction of cell death by phosphine silver (I) thiocyanate complexes in SNO-esophageal cancer cells. *Biometals*, 28, pp.219-228.
- Jenkins, S.R., 2014. Insights into the mechanism of drug action of a novel silver (I) chemotherapeutic against a malignant melanoma cell line. University of Johannesburg (South Africa).

APPENDIX B

B1.1 REAL-TIME QUANTITATIVE PCR DATA

Table B1.1 Concentration and absorbance ratios of RNA extracted from *E. xiangfangensis* Pb204 treated with silver(I) compounds.

Sample	Concentration (ng/ μ L)	A260/230 ratio	A260/280 ratio
Untreated control 1	1396.4	1.96	1.57
Untreated control 2	1258.3	2.04	1.99
Untreated control 3	360.3	2.03	1.78
UJ1 treated 1	504.5	1.96	1.82
UJ1 treated 2	176.8	1.99	1.78
UJ1 treated 3	346.9	2.15	1.50
AgSD treated 1	299.6	2.18	1.71
AgSD treated 2	1028.9	1.87	1.96
AgSD treated 3	172.1	1.94	1.93
AgNO ₃ treated 1	784.7	2.01	1.88
AgNO ₃ treated 2	647.0	1.89	2.01
AgNO ₃ treated 3	544.2	2.12	1.77

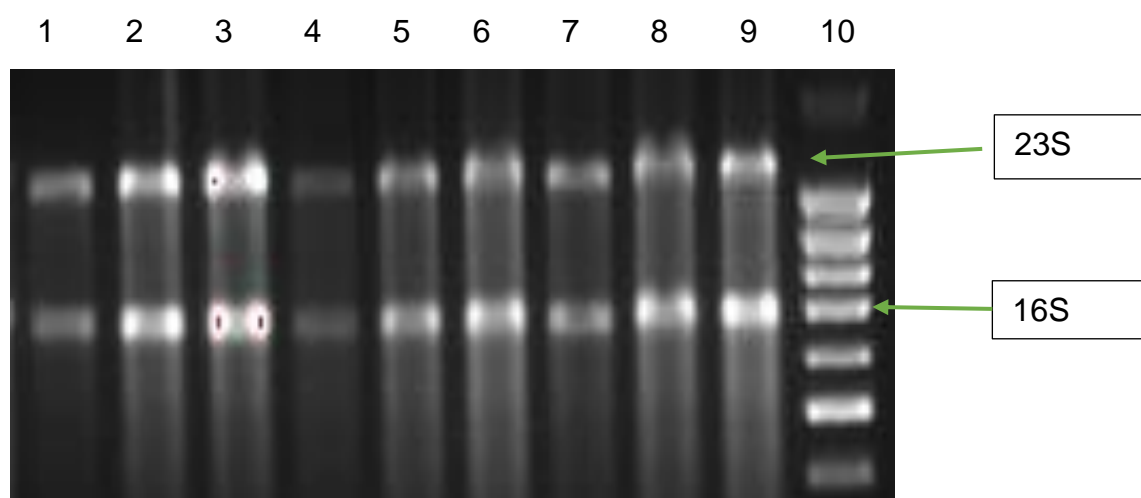


Figure B1.1: Agarose gel (1%) (w/v) showing the integrity of RNA extracted from *Enterobacter xiangfangensis* Pb204 cells treated with UJ1, silver nitrate and silver sulfadiazine. The cells were treated for 16 h prior to RNA extraction. The intact 23S and 16S unit is shown on lane 1 to 10, where the RNA is extracted from cells treated with UJ1 (lane 1 and 2), silver nitrate (lane 3 and 4), silver sulfadiazine (lane 5 and 6), untreated control (lane 7 and 8) and molecular weight marker (lane 10).